

REVIEW OF HEAT TRANSFER TO HELIUM I*

R.V. Smith
Cryogenics Division
NBS Institute for Basic Standards
Boulder, Colorado

I. INTRODUCTION

The purpose of this paper is to collect, compile, and to make useful recommendations on information with respect to heat transfer to helium I. The collection section of the paper considers all the relevant information with respect to helium heat transfer. This includes not only data on heat transfer coefficients but also appropriate properties data and heat transfer data, from systems using fluids other than helium, that should be useful to this study. The purpose of the compilation section of the paper will be to present these data in a concise manner which is optimally useful for engineering or design studies. The recommendations section of the paper will be concerned both with making recommendations for engineering and design practices on the basis of the findings of the first two sections of the paper and also with recommending future studies which are needed so that optimum design may be achieved.

II. HELIUM VERSUS CONVENTIONAL FLUID

At the outset, it might be well to consider the differences one may encounter between heat transfer studies with conventional fluids, such as air or water, and with a cryogenic fluid. First, as shown in Fig. 1 for helium, small pressure and temperature ranges enclose a given fluid phase or condition. Thus, for the pressure and temperature ranges required by some cooling systems one may encounter the helium fluid in a number of phases or states. Also, with helium the designer may be unable to avoid the regions around the critical point where the fluid behavior has some undesirable characteristics and where the heat transfer phenomena are not well understood. Therefore, when dealing with liquid helium, one must expect to encounter heat transfer problems which involve the liquid, the supercritical fluid, and also fluid in the two-phase condition. Certainly, the two phase and the supercritical fluid regions are among the more difficult heat transfer regions to study for any fluid. At helium temperatures there are no alternative fluids available.

Secondly, perhaps as great or even greater differences may be noted in comparing transport properties of a conventional and of a cryogenic fluid in which there is some quantum influence for any given phase. Figure 2 from Corruccini¹ shows the general differences in behavior of a conventional and a quantum fluid. In particular, one should note the behavior of the lower pressure liquid where the slope of the conductivity curve is reversed. The behavior might be expected to require, at least, a modification of a correlation developed for conventional liquids.

Even greater evidence of the difficulties of heat transfer studies with helium may be found on examination of Figs. 3, 4, and 5,² which show the viscosity and conductivity data available for helium at the present time. In considering helium heat transfer studies, one immediately notices the large regions indicated by the dashed lines where

*This work was carried out at the National Bureau of Standards under the sponsorship of the U.S. Atomic Energy Commission Contract Agreement AT(49-2)-1165.

there are no reliable experimental or theoretical guides and where values for properties must be considered to be crude estimates with a poor degree of reliability. Except for data in the saturated region and in the vicinity of 1 atm, the reliability of the data shown by the solid lines is marginal for use in heat transfer studies. Figures 4a and 5a show the data with constant-pressure parameters for engineering use. Thirdly, the values of the properties are relatively different from those of a conventional fluid. For example, at the normal boiling point the viscosity of water is about 100 times that of helium, the specific heat about equal to that of helium, and the density about eight times as great. Therefore, in considering the conventional heat transfer correlations which involve Reynolds ($uD\rho/\mu$) and Prandtl ($c_p\mu/k$) numbers, one can quickly see that, with helium, quite different combinations of values of these dimensionless groups will be encountered. Since the correlations themselves are not based on rigorous theory but are, indeed, primarily empirical relationships of dimensionless groups, the extensions of these expressions into regions where the fluid properties differ by such a margin cannot be justified without some experimental verification.

In summary, with respect to transport properties, heat transfer studies are more difficult because the properties vary significantly in value from those of conventional fluids, and extrapolation of the correlations are not justified without experimental verification. Further, the transport properties for the liquids behave quite differently from those of conventional fluids except at very high pressures, and the reliability of all of the properties data leaves a great deal to be desired in pursuing heat transfer studies. Finally, heat transfer studies with helium are substantially more difficult than those dealing with conventional fluids because one must deal with the difficult regions for heat transfer with respect to phase changes and pseudo-phase changes. The problem is additionally complicated by marked differences in behavior and in values of the transport properties from those of conventional fluids, and by a poor reliability of data for these transport properties.

III. DIVISION INTO REGIONS OF PHASE AND TRANSPORT PROPERTY BEHAVIOR

In general, one might say that heat transfer phenomena are influenced by two sets of conditions. One set of conditions has to do with the physical properties and the other with the flow structure. With respect to the flow structure, one is primarily concerned with the behavior in the boundary layer. That is, one would first want to know whether the boundary layer is laminar or turbulent and, if turbulent, the nature of the turbulence. Since the flow structure is very much a function of a specific system, it was decided not to make any divisions in this study with respect to this phenomenon. Therefore, the heat transfer study of helium will be divided into regions with respect to the transport property and phase behavior, and the characteristics of the flow structure will be discussed in these regions where appropriate. The divisions are shown in Fig. 6.

Region 1 and Region 2 differ from each other primarily because in Region 2 phase separation with equilibrium will be distinct whereas in Region 1 phase separation is either not distinct or not possible. The liquid region and the gaseous region are Regions 3 and 4, respectively.

The line of maximum specific heats, which separates Region 1 from Region 4, is quite significant because, on the left of the line, one has what is often called a pseudo-liquid. In this region then, quite close to the saturated liquid line or the line of maximum specific heats, one does experience pressure and density oscillations and other phenomena which are usually associated with the two-phase region.

The data from which these curves were constructed may be seen in Fig. 7a.³ In Fig. 7a the constant-pressure lines show distinct peaks or humps in the specific heat behavior for pressures reasonably close to the critical pressure. The maximum points

of these peaks constitute the locus of points used to construct the maximum specific heat or "transposed critical" curve. The dashed line in Fig. 6 representing this condition is drawn with shorter dashes as the pressure is increased to indicate a weaker tendency toward critical-point behavior. In drawing the line in this manner it was meant to show that, as the peaking of the specific heat curve became less distinct, the line, while still indicating the maximum specific heats, was recording a phenomenon which was becoming less and less important. Fluid in conditions falling to the left of this maximum specific heat curve is often called a pseudo-liquid, with fluid on the right of this maximum specific heat curve similarly named a pseudo-gas. Further two-phase analogy is seen in Fig. 7b,⁴ from which large density changes associated with the crossing of the transposed critical line can be deduced.

Looking at the regions from the point of view of heat transfer knowledge obtained from other fluids, one might make some general statements as to the expected behavior for each of the regions selected. In Region 4, the gas region, one would expect the conventional correlations to be generally effective although some modification may be required because of the properties behavior previously discussed. In Region 3, the liquid region, the properties behavior with respect to that of conventional fluids is quite different; however, the conventional correlations should still form the basis by which one may make reliable heat transfer predictions. Heat transfer phenomena in Region 2, the two-phase region, is not well understood for any fluid. This means that almost any extension of the use of conventional expressions to the helium region should be accompanied by a rather complete experimental verification if any substantial reliability is required in the use of the data. In Region 1 the pseudo-liquid or supercritical region near the line of maximum specific heats, a poor understanding exists, at best, for the heat transfer behavior. Here again, a good deal of experimental data will be required for helium if reliable heat transfer predictions are to be achieved.

IV. REGION 1 - SUPERCRITICAL NEAR THE TRANSPOSED CRITICAL LINE

IV.1. Region Boundaries

Referring to Fig. 6, one may see that the best defined boundary for Region 1 is that made by the line of maximum specific heats or the transposed critical line. The transport properties of viscosity and conductivity are generally believed to go through a similar peaking phenomenon as shown in Fig. 7a when the critical point is approached for any fluid. Therefore, it would be expected that curves similar to Fig. 7a could be generated, for helium, for the transport properties of conductivity and viscosity. However, no experimental data have been generated to verify this concept.

The left boundary of this region is more difficult to define. It is meant to describe the boundary such that the fluid on its left shows no evidence of maxima singularities in its properties nor associated tendencies toward pressure oscillations. One might conclude, therefore, that the left boundary of this region should fall along a pressure line where the specific heat curve as shown in Fig. 7a no longer exhibits a peaking behavior or the density curve shown in Fig. 7b no longer has a steep slope. For helium, this would appear to be along a constant pressure line in the region of roughly 15 atm.

It might be reasoned that Region 1 should extend to the right of the transposed critical line as well as to the left. This area includes the right half of the property "hump" behavior shown in Fig. 7a. For this paper, it was decided not to include this area in Region 1 for two reasons. First, the slope of the curves describing property behavior are less steep on this side of the maxima. Secondly, almost all heat transfer processes which seem likely with helium involve pressure reduction. Consequently processes will generally run from left to right in Fig. 6. Therefore, the variable property region is unlikely to be approached from the right of the transposed critical line.

The lower boundary of the curve which extends across the liquid-vapor dome is also reasonably difficult to define in a precise or distinct manner. The curve is intended to form a boundary such that fluid which falls above the curve will have properties, particularly density properties, for the liquid and the gas such that a separation of the phases is fairly slow or difficult.

IV.2. Behavior of Conventional Fluids in Region 1

In Region 1, the special problem encountered in the heat transfer analysis is that of the fluid property, particularly the transport and density property, behavior in the boundary layer. These variations are shown in Figs. 7a and 7b. If the wall temperature is above the transposed critical temperature for the fluid and the bulk temperature of the fluid below that value, some fluid in the boundary layer must be in Region 1. This means that there will be widely varying values for the properties and, also, situations where some of the properties will go through maximum values within the boundary layer. Most heat transfer correlations assume the use of constant or effective property values. Correlations using this system are known to be ineffective for conditions where there are wide variations in the fluid boundary layers. This would occur either when there are high temperature differences between the wall and the fluid or when there are large property variations with relatively small variations in temperature such as those conditions in Region 1.

IV.2.1. Oscillations

Perhaps the most important physical phenomenon which has been associated with this region has been that of pressure and flow oscillations. This behavior has been similar to that of a two-phase fluid. Some authors have chosen to label this as a boiling-like or a pseudo-boiling region. Among these are Dickinson and Welch,⁵ Dubrovina and Skripov,⁶ and Griffith and Sabersky.⁷ One might very easily associate this phenomenon with the presence of a heavy and light species in this region; however, this has not been completely experimentally documented at this time. Some understanding of these oscillations has been obtained by the use of treatments that are modifications of rather conventional mechanics developed to describe specifically the oscillating systems. That is, the fluid system has been treated as one which is analogous to a more conventional oscillating system. Among those papers that have recently reported studies primarily dealing with oscillations in this region are the following: Hendricks et al.⁸ for hydrogen, Thurston et al.⁹ and Thurston^{10,11} for hydrogen, and Cornelius¹² for Freon 114.

IV.2.2. Temperature profiles in the boundary layer

Some further insight into the behavior in the fluid in this region may be obtained by consideration of the temperature profiles one might expect to find in the boundary layer. This was investigated by Wood and Smith¹³ using carbon dioxide. First of all, one does not expect to find these phenomena occurring except when the transposed critical temperature falls between the temperature of the wall and the temperature of the bulk of the fluid. When these conditions are met, then, of course, the extreme behavior of the fluid properties will be found in the region of the boundary layer. Most papers record that this special behavior indeed does occur only when these temperature conditions are met. Some further insight into the behavior of the temperature profiles in the boundary layer may be found by first considering the expression for turbulent heat transfer which is as follows:

$$q/A = (k + \epsilon_h \rho C_p) \frac{dT}{dy} \quad (1)$$

In the parentheses, the first term describes heat transfer coefficient of the temperature

gradient that would exist if the boundary layer were completely laminar, while the group of terms in the parentheses represents the coefficient of the gradient for the turbulent condition. Remembering that in all flow there is a laminar-like sublayer, one might speculate that, in this region where the conductivity term controls, and where this value will be expected to be enhanced generally, the resistance to heat transfer would be decreased and the temperature profile would be less steep than usual in this region. If the turbulent level or scale of turbulence is assumed to be essentially constant, then the resistance to heat transfer in this region will be inversely proportional to the density times the specific heat. In examining the terms in this region one would generally expect the resistance to decrease. This is because the specific heat would be expected to increase more rapidly than the compensating density decrease near the critical point.

Another possible change in the heat transfer in this region might be brought about by a change in the level of turbulence shown by ϵ_h . Such a change may be possible because the large density changes shown in Fig. 7b would create a rather large fluid acceleration. Under such circumstances the turbulent eddies might change such that the level of turbulence would be reduced.

IV.2.3. Behavior of the heat transfer coefficient

Then, looking at these two regions of the laminar sublayer and the turbulent core, one finds that the resistance in the net is decreased in the laminar sublayer and in the turbulent core so that the conventional temperature profile would be somewhat flattened for this heat transfer condition. Considering these circumstances alone, one might expect the heat transfer in the net to be enhanced because of these changes in this region. After the bulk temperature reaches the transposed critical temperature, however, the opposite would be expected to be true and one would expect to find a degradation of the heat transfer rate. This is indicated by property behavior and confirmed by experiment.

An example of this behavior of the heat transfer coefficient near the transposed critical is shown in Figs. 8a and 8b as reported by Dubrovina and Skripov.⁶ These figures show that the heat transfer coefficient follows the property behavior rather closely, with a substantial enhancement near the transposed critical and considerably lower values on either side. It should be noted, however, that Fig. 8b shows that the enhancement occurs only for very small temperature differences between the wall and the fluid.

IV.3. Analytical Work

Finally, one may consider the analytical work which has been reported to describe the heat transfer in this region. One may generally arrange this work into two sections divided by the general method of approach which was used. One set of analyses has concerned itself with an integration through the boundary layer for the case of variable fluid properties. This method involves the use of universal parameters for the flow variables. A review of universal velocity distribution functions may be found in Spalding.¹⁴

Deissler^{15,16} has presented a series of papers employing this method. Figure 9 shows the relationship between the temperature, T_x , at which properties are evaluated to produce the proper relationship between the Nusselt number and the Reynolds number for supercritical water. These curves are for a Prandtl number of one. Of course, some function of the Prandtl number can be found to bring the curves nearer to a single curve. One may also see that if the proper temperature, T_x , is chosen the same form of the conventional correlation which employs constant properties may be used.

The other method of analyzing experimental data reported in this region is to seek a satisfactory modifying parameter for the conventional correlations. In almost all the cases, this modifying parameter contains the ratio of the wall to bulk temperature or the ratio of properties which are primarily a function of this temperature ratio, such as kinematic viscosity. Thus,

$$Nu = 0.023 (Re)^{0.8} (Pr)^{0.4} \text{ (modifying parameter)}$$

where

$$\text{(modifying parameter)} = (T_w/T_b)^{(a)} \text{ or } f(\nu_w/\nu_b)$$

where a is an exponent determined empirically.

Hendricks et al.¹⁷ show a ratio of the Nusselt number over a Nusselt number calculated by an analogous procedure to a two-phase Nusselt number correlated with the Martinelli and Nelson¹⁸ parameter as

$$\frac{Nu}{Nu_{calc}} = f(x_{tt})$$

Again, the correlations produced by this method have been shown to be superior to those simply using the conventional single-phase heat transfer correlations.

Although the two methods of approach previously discussed appear to be quite different, the resulting correlations are fairly similar in form. Some examples of these predictive correlations and their use follow:

Bringer and Smith¹⁹ Forced Convection CO₂ (no humps)

$$Nu = 0.0266 (Re)_{T_x}^{0.77} (Pr)_{T_x}^{0.55} \text{ (Deissler}^{15})$$

Wood and Smith¹³ Forced Convection CO₂ - Two resistance concept - Enhanced near transposed critical

Miller et al.²⁰ and Miller²¹ Forced Convection H₂ (no humps)

$$Nu = 0.0204 \left(\frac{\rho_{0.4} u_b^D}{\mu_{0.4}} \right)^{0.8} (Pr)_{0.4}^{0.4} (1 + 0.00983 \nu_w/\nu_b)$$

where the subscript indicates the location of the boundary layer temperature for the property evaluation as proposed by Deissler and Pressler²² and the modifying parameter is of the form proposed by Hess and Kunz.²³

IV.4. Helium I in Region 1

Three papers have reported on systems which involved heat transfer to supercritical helium. These are: Kolm et al.,⁴ Klipping and Kutzner,²⁴ and Brechna.²⁵ Because the actual boundaries of Region 1 are yet to be determined, it cannot be said whether or not these data actually have fallen in what has been termed Region 1 for this paper. Additionally, all of these papers which do report data are handicapped because reliable property data are lacking in this general region for helium. Kolm et al.⁴ reports a system using the supercritical helium I for heat transfer but does not report experimental heat transfer data. Klipping and Kutzner²⁴ report a study of heat transfer to supercritical helium by free convection. The heated surface was a horizontal cylinder,

2 cm long and 0.4 cm in diameter. Since property data were not available, they reported the data in a form as shown in Fig. 10. Here, one can see that, as Kolm et al.⁴ had previously suggested, heat transfer with supercritical helium is competitive with boiling heat transfer from other fluids and also with boiling heat transfer from helium. Brechna²⁵ shows some results from forced convection heat transfer using superconductor cable material. These results indicate that the helium heat transfer in this region is about 1.7 times that which would be expected using conventional single-phase heat transfer correlations. This work is also discussed for Region 3.

The very limited reported data for heat transfer to supercritical helium I do not allow any conclusions except that more work is certainly needed in this region. For optimum design of any system employing heat transfer to supercritical helium, one first needs the necessary transport property data, and secondly, one needs reliable predictive heat transfer correlations for the fluid. It would appear that these correlations will be modifications of the correlations applied to conventional fluids. Additionally, the boundaries of Region 1 need to be defined rather specifically. This is particularly important with respect to pressure and temperature oscillations. In heat transfer to cool superconductors, stability is much more important than in ordinary heat transfer situations. Therefore, the unstable regions where pressure oscillations might occur with supercritical helium need to be well defined.

V. REGION 2 - TWO-PHASE, BOILING HEAT TRANSFER REGION

The accepted divisions of boiling studies into that of pool boiling and forced convection boiling will be made.

V.1. Pool Boiling

V.1.1. Boundaries of regions

The boundaries of this region seem reasonably well defined. Referring again to Fig. 6, the left boundary is in the vicinity of a liquid-vapor saturation line. Some further discussion of the point of inception of bubbles will be carried out in the subsequent examination of the boiling curves. The lower limit of the region is in the vicinity of the lambda line. The right hand division of the region is distinct, as the vapor saturation line. Finally, the upper limit of the region has been discussed previously since it forms the boundary of the lower part of Region 1.

V.1.2. Behavior of conventional fluids - pool boiling

The general boiling curve exhibited for all fluids may be divided into four sections of study. These are:

- The nucleate boiling curve.
- The maximum nucleate boiling flux.
- The film boiling curve.
- The minimum film boiling flux.

Following the pattern set in Region 1, the behavior of other fluids in these various boiling divisions will be discussed first. This will allow some insight into the peculiarities of helium boiling and allow estimates for helium behavior where data have not been previously obtained or have been obtained in very small quantities without the confirmation of subsequent studies.

V.1.2.1. Nucleate boiling

Typical nucleate boiling curves may be seen in Figs. 11, 13, and 14. The lower portion of the curve is defined by the inception of the formation of bubbles and on a plot such as in Figs. 13 and 14 where the heat transfer per unit area is plotted against the temperature difference between the bulk of the fluid and its surface, the inception of bubbles causes a sharp rise in the slope of the curves. This slope remains generally constant on such a plot and is proportional to about the third power of the temperature difference. The analytical curves then developed to express the nucleate boiling phenomena will be of the general form

$$q/A = f_{(\text{properties})} (T_w - T_{\text{sat}})^3 \quad (2)$$

It seems reasonably well established at this time that, in many cases, the multiplier of the temperature difference is a function of the heated surface as well as the fluid. This aspect of boiling will be discussed in a later section.

A number of nucleate boiling curves, evaluated for hydrogen at 1 atm, are shown in Fig. 11 along with the regions of reported experimental data. In general, the correlations are dependent upon fluid properties alone, and that will be the basis on which these curves will be discussed. The state of knowledge regarding the boiling phenomena has not advanced to the point where the primary or controlling influences in the process have been established in a manner generally accepted as that one which is correct. Therefore, all of the correlations may be said to owe some of their development to dimensional or similarity concepts. A number of the correlations that have been more recently proposed involve the number of nucleation sites. Since these data are not generally available on an engineering or design basis, these correlations are not yet useful for design use. In a previous report on boiling of cryogenic fluids by Brentari and Smith,²⁶ the Kutateladze²⁷ correlation was recommended as one that represented the behavior of hydrogen reasonably well. Obviously, from an examination of Fig. 11, one can see that several other correlations could be said to represent the data with equal reliability. The general requirements for a successful correlation are to express the properties data in such a way that the curve will have a point with the approximately correct horizontal location and then from that point have the slope expressed as about the third power of a temperature difference. Since the Kutateladze correlation is reasonably successful for the cryogenic fluids it will be used as a reference in the subsequent discussion of helium boiling. This expression is

$$\frac{h}{k_l} \left(\frac{\sigma}{g \rho_l} \right)^{\frac{1}{2}} = 3.25 (10)^{-4} \left[\frac{(q/A) (C_p)_l \rho_l}{h_{fg} \rho_v k_l} \left(\frac{\sigma}{g \rho_l} \right)^{\frac{1}{2}} \right]^{0.6} \quad (3)$$

$$\left[g \left(\frac{\rho_l}{\mu_l} \right)^2 \left(\frac{\sigma}{g \rho_l} \right)^{3/2} \right]^{0.125} \left[\frac{P}{(\sigma g \rho_l)^{\frac{1}{2}}} \right]^{0.7}$$

V.1.2.2. Maximum nucleate boiling flux

As the temperature of the heated surface is increased during nucleate boiling a point is reached where the nucleate boiling curve essentially becomes discontinuous. Physically, this might be very roughly visualized as the point at which the vapor removal procedure during the boiling becomes such that a wetting cycle during that process is no longer possible. The boiling is then said to enter the film boiling regime where essentially a vapor film is maintained between the heated surface and the bulk of the liquid. This point is almost always associated with a very rapid increase in the temperature of the heated surface. The point is of particular interest to many

design situations because, very often, if this condition is allowed to occur, it will result in the system's failure. This would almost certainly be the case for a helium-cooled superconductor. In separate studies, both Kutateladze²⁷ and Zuber²⁸ have produced expressions which are reasonably successful in predicting this maximum flux. This expression is as follows:

$$(q/A)_{\max} = 0.16 h_{fg} \rho_v^{1/2} \left[\sigma g (\rho_l - \rho_v) \right]^{1/4} \quad (4)$$

Again, it will be noted that this expression is a function of a fluid properties alone and not of the relationship between the fluid and the boiling surface conditions or of the surface conditions. Deviations which may occur as a result of the surface conditions will be discussed subsequently in this section. It should be pointed out that although the maximum heat flux can be predicted to a reasonable degree of accuracy, the temperature difference at which this flux will occur is much more difficult to predict. One may estimate this temperature difference by using the value of the maximum heat flux substituted in the nucleate-boiling-curve correlation.

Figure 12 shows the values obtained from (4) compared with experimental data from cryogenic fluids. The agreement is reasonably good except for lower values of the abscissa which correspond to higher values of p/p_c .

V.1.2.3. Film boiling

Typical film boiling curves produced from experimental and analytical data may be seen in Fig. 13. Again, in a previous review by Brentari and Smith,²⁶ the Breen and Westwater²⁹ correlation was found to describe the behavior of cryogenic fluids boiling in the film region reasonably well. Therefore, most of the discussion relating analytical to experimental work in this paper will be referred to that correlation. In order to calculate the heat transfer in the film boiling region one must know something of the characteristics of the film or make some assumptions regarding these characteristics. Most of the more recently proposed analyses study the stability of the liquid-vapor interface of this film. This was the approach of Bromley³⁰ and subsequently of Breen and Westwater²⁹ who presented the following correlation:

$$h \left(\frac{\sigma}{g(\rho_l - \rho_v)} \right)^{1/8} \left[\frac{\mu_v (T_w - T_{\text{sat}})}{k_v^3 \rho_v (\rho_l - \rho_v) g h'_{fg}} \right]^{1/4} = 0.37 + 0.28 \left(\frac{\sigma}{g D^2 (\rho_l - \rho_v)} \right)^{1/2}, \quad (5)$$

where

$$h'_{fg} = \frac{[h_{fg} + 0.34 C_{p,l} (T_2 - T_l)]^2}{h_{fg}}$$

It should be noted that a diameter effect does occur in the correlation, but otherwise surface effects are considered negligible.

V.1.2.4. Minimum film boiling flux

In proceeding downward along the film boiling curve, as $(T_w - T_{\text{sat}})$ is reduced, there will be a point reached when the boiling mechanism will return to nucleate boiling. This point at which that change occurs is known as the minimum film boiling flux. This point is also of considerable interest to designers because it represents the minimum heat flux which would be expected in the temperature range of nucleate and film boiling except, perhaps, for cases of very low temperature differences on the nucleate boiling curve. Several authors, among them Zuber,²⁸ and Lienhard and Wong,³¹ have produced predictive equations for the minimum film boiling. This point is quite difficult

to obtain experimentally, and specific experimental information on this heat flux is reasonably scarce for any fluid. The point, however, can be generally determined for most fluids from a knowledge of the necessary shape of the general boiling curve and from data regarding the nucleate and film boiling regions. The correlation proposed by the two authors previously mentioned has been shown to be reasonably successful for other cryogenic fluids. This correlation for a cylinder with $D > 1.0$ cm or for a flat plate is:

$$(q/A)_{\min} = 0.16 h_{fg} \rho_v \left[\frac{g \sigma (\rho_l - \rho_v)}{(\rho_l + \rho_v)^2} \right]^{1/4} \quad (6)$$

V.1.2.5. General discussion of the boiling correlations

In many cases, additional factors should be considered before the previously discussed correlations are used to predict the behavior of a system. The correlations are primarily limited because, for wider variations in fluid properties, the correlations have not been thoroughly tested and some tests show poor reliability at high values p/p_c ; further, they do not account for the geometry or the properties of the solid surface.

V.1.2.5.1. Nucleate boiling correlations - pressure effects

Both the expressions for the nucleate boiling flux (3) and the maximum nucleate flux (4) appear to be unreliable at $p/p_c > 0.6$. (See Figs. 15 and 16.)

V.1.2.5.2. Subcooling

When temperatures of the liquid are below the saturation temperatures, the boiling fluxes are changed from those indicated in the previous discussion where only saturated liquid conditions were considered. Four expressions have been proposed as a correction to the expressions that consider saturated liquids. The correction is simply

$$(q/A)_{\substack{\text{subcooled} \\ \text{max}}} = (q/A)_{\substack{\text{sat} \\ \text{max}}} F_{\text{sub}} \quad (7)$$

These expressions are:

Kutateladze I²⁷:

$$F_{\text{sub}} = 1.0 + 0.040 \left(\frac{\rho_l}{\rho_v} \right)^{0.923} \left(\frac{C_p}{h_{fg}} \right) (T_{\text{sat}} - T_{\text{sub}}) \quad (8)$$

Kutateladze II (from Gambill³²):

$$F_{\text{sub}} = 1.0 + 0.065 \left(\frac{\rho_l}{\rho_v} \right)^{0.800} \left(\frac{C_p}{h_{fg}} \right) (T_{\text{sat}} - T_{\text{sub}}) \quad (9)$$

Ivey and Morris³³ (from Gambill³²):

$$F_{\text{sub}} = 1.0 + 0.102 \left(\frac{\rho_l}{\rho_v} \right)^{0.750} \left(\frac{C_p}{h_{fg}} \right) (T_{\text{sat}} - T_{\text{sub}}) \quad (10)$$

Zuber et al.³⁴:

$$F_{\text{sub}} = 1.0 + 12.326 \left[\frac{(C_p \rho_k)_l^{0.500} (\Delta p)^{0.125}}{h_{fg} \rho_v^{0.750} \sigma^{0.375}} \right] (T_{\text{sat}} - T_{\text{sub}}) \quad (11)$$

There are no experimental data to test these expressions for cryogenic liquids.

V.1.2.5.3. Surface conditions

While it is known that surface conditions have a significant effect on the boiling phenomena, the specific influence of any given surface variable is not well understood. Enough data have been acquired, however, to permit a qualitative discussion of the effects of specific surface variations. Considered here are surface history, surface temperature variations as affected by the heated material mass and properties or by the type of heat source, surface roughness, and surface-fluid interface phenomena as influenced by the surface and fluid chemical composition.

V.1.2.5.3.1. Surface history

A heating surface immediately after immersion in liquid will produce a higher heat transfer coefficient than one which has been immersed for a reasonable period of time (Kutateladze²⁷). This is presumably due to additional nucleation centers provided by factors such as dissolved air and oxidation of the heating surface. Graham et al.³⁵ reported that for nucleate boiling of hydrogen, boundary layer history has a significant effect on the boiling incipient point. The apparent incipient point for nucleate boiling occurred at a much lower ΔT when a boiling run was immediately repeated rather than begun with a fresh supply of hydrogen surrounding the heating surface; the two curves then join at higher heat fluxes. The authors speculate that some residue of the thermal layer remained to change the incipient point for the succeeding test.

Vliet and Leppert³⁶ studied the effect of aging or boiling for a period of time at about half peak flux. They found that with water flowing over a stainless-steel tube, aging of about 90 min was necessary before reproducible peak fluxes could be obtained. Aging for about one-third that time produced peak fluxes only slightly greater than half the fluxes produced using the longer aging procedure.

V.1.2.5.3.2. Surface temperature variations

It is possible that surface temperature differences can occur which may be attributed to properties of the heater surface and not entirely to the fluid boiling phenomena. Heaters with a small mass per unit of heater surface such as very thin materials may produce temperature variations and, subsequently, a lower peak flux. Vliet and Leppert,³⁶ however, reported that there were no surface effects down to a thickness of 0.006 in. for a cylinder with water cross-flow.

The source of energy for the heater may also influence surface temperature variations. Kutateladze²⁷ reports that electrically heated surfaces have slightly different heat transfer characteristics than those heated by vapor condensation, probably because condensation droplets cause surface temperature differences.

Of course, the boiling phenomena also produce temperature variations at the surface, and these are reported, for example, by Kutateladze,²⁷ Hendricks and Sharp,³⁷ and Moore and Mesler.³⁸ Sharp³⁹ studied the microlayer film at the base of nucleate bubbles and found that the flux from this microlayer appeared to vary with $k/\sqrt{\alpha}$ for

the surface material. Cummings and Smith,⁴⁰ and Bowman,⁴¹ have shown some boiling variations which are a function of the properties of the substrate material, and in turn, may be attributed to changes in these properties during temperature fluctuations.

V.1.2.5.3.3. Surface roughness

Rougher surfaces generally produce higher fluxes for the same ΔT . Mikhail⁴² reported work with oxygen using nickel surfaces with different roughness values, and his data were similar to others who investigated higher temperature fluids. Rougher surfaces cause incipient nucleate boiling to occur at a lower ΔT , and then the h vs ΔT curves rise abruptly from that point. Thus the rougher surfaces produce markedly higher coefficients for the same ΔT - in Mikhail's work as high as a factor of 4. Lyon,⁴³ working with cryogenic and other liquids, indicates, however, that although the nucleate boiling flux curve is changed by roughness, the peak flux does not change. Surface roughness would be expected to show a much smaller effect in the film boiling region, and work such as that of Class et al.⁴⁴ indicates essentially no effect of roughness for film boiling.

Tuck,⁴⁵ in experimental work with hydrogen, found that ΔT for inception was less than 0.1°K for a rough surface but could be as great as 3°K for a surface finished to $1.25 \mu\text{in. rms}$. The Tuck experiments were at zero gravity condition; however, the results would be expected to be applicable generally under other gravitational fields, although at or near zero gravity the inception point seems to be time dependent and that time a function of the gravitational field.

V.1.2.5.3.4. Surface chemistry

The surface chemical effect is often difficult to separate from other surface effects such as roughness. Wetting characteristics would appear to be a major influence. Cryogenic fluids will wet almost all surfaces except those with a very low surface energy; this is illustrated, for example, in a hydrogen study by Good and Ferry⁴⁶ and perhaps further substantiated by the reasonably effective use of a single wetting coefficient in the Rohsenow⁴⁷ correlation for cryogenic fluids. Lyon⁴³ studied nucleate boiling with oxygen and nitrogen using clean copper and gold surfaces and surfaces with various chemical films. He found that the different surfaces produced somewhat different nucleate boiling curves and differences as much as 25% in the peak flux.

Young and Hummel⁴⁸ have shown that higher coefficients in the lower region of the nucleate boiling regime are made possible by providing poorly wetted spots on the metal surface. Sharp³⁹ has studied the microlayer at the base of bubbles and has found that nonwetting surfaces tend to destabilize the layer. Costello et al.⁴⁹ found that the burnout heat flux was increased by a factor of 2.3 if tap water rather than distilled water was used.

V.1.2.5.4. Geometry

The correlations essentially describe systems of simple geometry with surfaces which are vertical or facing upward. The data from the surfaces facing downward and of vertical channels are shown in Figs. 18 and 19 which will be discussed later. Other variations with geometry have been reported; for example, Costello et al.⁴⁹ have reported that for pool boiling burnout heater size is quite significant. They found that 0.067 in. diameter semi-cylinders burned out at fluxes 2.7 times greater than for flat plate heaters with no liquid in-flow from the sides. This suggested to the authors that such difference may be a result of different convective effects for the various heated surfaces. They show that the convective component may be approximately one-half the total flux in some cases.

V.1.3. Pool boiling - helium I

V.1.3.1. Comparison of data with results from correlations

Figure 13 shows experimental and analytical pool boiling data for helium. The figure indicates that agreement between the predictive correlations and the experimental work is approximately as good as that for other fluids. In order to show most of the reported experimental work, some of the data have been corrected by means of the property variations indicated by (3) to the case for $\frac{1}{2}$ atm pressure. These data are for simple geometries with surfaces facing upward or vertical.

Figure 16 shows the comparison of the results of the maximum nucleate flux comparisons. Here, as with the other cryogenic fluids, the agreement is good except for higher values of p/p_c . It would appear that a safe upper limit for the correlation would be $p/p_c = 0.6$.

V.1.3.2. Pool boiling - additional factors to consider with the correlations

V.1.3.2.1. Hysteresis

Figure 14 shows the hysteresis effect as reported by three investigators. The difference in the curves with increasing flux and decreasing flux is generally regarded as being associated with the point of initial bubble inception and its requirements for higher temperatures than that for subsequent bubbles. Also, as the temperature differences and the heat fluxes are increased the behavior of the curve must indicate the activation of new boiling sites.

Bankoff⁵⁰ has shown that, in general, the theoretical superheat requirements to form new vapor nuclei are considerably higher than those observed. Therefore, one might conclude that nucleation usually occurs at nonwetted sites on the surface, usually in cavities. This hypothesis could be used to explain the additional hysteresis for helium because at helium temperatures all gases which might serve to create nonwetted sites will be condensed, except helium itself.

V.1.3.2.2. Geometry effects

Figure 17 shows data from two sources for surfaces facing downward. In both cases the data appear to follow the same general nucleate boiling behavior except that the maximum flux is reduced very substantially.

The work of Sydoriak and Roberts⁵¹ for narrow channels shows that for this special geometry, the helium boiling problem must be handled quite differently. They developed an expression for the maximum flux which, for this case, is limited by the outflow rate from the channel. Figure 19 shows the predicted results from this theory compared with experimental data from Wilson.⁵² The agreement appears reasonably good, particularly for a problem as complex as this one.

Figure 13 indicates that the film boiling correlation (5) does not properly account for boiling behavior with small wire sizes.

V.1.3.2.3. Substrate effects

Figure 20 shows the results of Cummings and Smith⁴⁰ which demonstrate significant effects traceable to the behavior of the properties of the substrate. These properties are conductivity, density, and specific heat. The authors show that these properties, together with a frequency term (representing boiling bubble frequency), can be made to

form a function that will correlate boiling data from different substrates. This behavior could well be most significant for helium because the properties will tend to vary more with small temperature changes (such as those encountered in boiling) at helium temperatures.

Bowman⁴¹ has shown that radiation has a significant influence on the pool boiling of helium by decreasing the thermal conductivity of the substrate and by inducing residual radioactivity in the substrate.

V.1.3.3. Additional factors to consider with correlations - significant but apparently no different for helium than for other fluids

V.1.3.3.1. Pressure

Figure 15 shows the nucleate boiling data of Lyon⁵³ taken at different pressures. The lower pressure data appear to behave essentially as predicted, but the higher pressure data are quite different from a reasonable extrapolation of lower pressure data or from the apparent prediction using (3). It may be that the property values used in (3) near the critical would be quite unreliable, but even with a reasonable allowance for that, one must conclude that the behavior indicates an approach quite different from (3) should be taken to predict the higher pressure behavior. As in the case of the maximum nucleate flux data (Fig. 12), it would appear that the correlations are only reliable to $p/p_c = 0.6$.

V.1.3.3.2. Surface roughness and chemistry

There are no reported studies which have considered surface chemistry effects. As previously discussed, Lyon⁴³ found significant effects for other cryogenic fluids.

Figure 17 shows surface roughness effects reported by Boissin et al.,⁵⁴ and Cummings and Smith.⁴⁰ The work of Boissin et al.⁵⁴ indicates that only polished surfaces are markedly different for the nucleate boiling curve. Cummings and Smith⁴⁰ show that ice crystals did not influence the nucleate boiling curve for their surface. They did, however, very significantly influence the curve in the region of transition from nucleate to film boiling.

V.1.3.3.3. Subcooling

There are no data to show the influence of subcooling (fluid temperatures below saturation) on helium boiling. Some indication of the possible effect can be obtained by evaluating (8)-(11) previously discussed. These evaluations are shown in Fig. 21.

V.2. Forced Convection Boiling

V.2.1. Behavior of conventional fluids

The general treatment of forced convection boiling is simply to extend the method used in the single-phase case. The systems employed may be divided into two general categories. In the first category a two-phase Nusselt number is calculated from a Dittus-Boelter⁵⁵ form of the equation

$$(\text{Nu}_{\text{calc}})_{\text{tp}} = 0.023 (\text{Re})_{\text{tp}}^{0.8} (\text{Pr})^{0.4}$$

In this equation the two-phase aspect is introduced by some sort of a two-phase modification of the density term in the Reynolds number. This Nusselt number does not yield

the proper film coefficient to describe the forced convection boiling process, however. Instead, it is used as the denominator of a Nusselt number ratio with the numerator representing the experimental or in the case of a predictive use of the correlation, the predictive Nusselt number. In this system the Nusselt number ratio is assumed to be a function of some correlating parameter. The most common correlating parameter employed is the Martinelli-Nelson parameter χ_{tt} which was originally proposed to correlate a similar pressure drop, or essentially a momentum transport process:

$$\text{Nu}/(\text{Nu}_{\text{calc}})_{\text{tp}} = f(\chi_{tt})$$

Hendricks et al.¹⁷ have reported a very thorough study employing this type of correlation using hydrogen as the working fluid. Figure 22⁵⁶ shows that the correlation is relatively successful for hydrogen.

The second analytical method, which is employed to describe forced convection boiling processes, is usually called the superposition method. Here, the concepts are very simple. The heat flux which would be indicated for the pool boiling case is simply added to the heat flux which would be indicated by a conventional correlation for the single phase fluid:

$$(q/A)_{\text{Forced conv. boiling}} = (q/A)_{\text{Pool boiling}} + (q/A)_{\text{Forced conv. single phase}}$$

For the case of nucleate boiling the single-phase fluid would be assumed to be a liquid, and for the film boiling case the single-phase fluid would generally be assumed to be a gas. Although this method is extremely simple and makes no provision at all for the interplay between the two energy transport processes, it has been shown to be reasonably successful for a number of fluids including hydrogen. Giarratano and Smith⁵⁷ have reported a comparative study of these methods using previously reported data for hydrogen heat transfer.

V.2.2. Forced convection boiling with helium I

There has only been one paper on forced convection boiling with helium. This is by de La Harpe et al.⁵⁸ who employed a long coiled tube. The authors used the method of a Nusselt number ratio correlated with the Martinelli parameter for their data with higher quality, higher vapor content, runs. Their results are shown in Fig. 23. This method produced an empirical line which correlated the data to within $\pm 20\%$. For the low quality region (where the quality was approximately 0.2 and less), the method of superposition was employed as the Nusselt number ratio appeared to be insensitive to changes in the Martinelli parameter for the low quality case. When the superposition method for the lower quality region was used, the data were correlated within $\pm 20\%$ for the range of experimental data produced. This dividing point between the apparent wet-wall and dry-wall regions is at a considerably higher quality than that which would be expected for other fluids. This is because the density ratio (of liquid to gas) at the normal boiling point for helium is much lower than that for other fluids. For example, for hydrogen this ratio is about 53 and for helium about 7.5. Wright and Walters⁵⁹ report wet-wall boiling data for a similar case of forced convection with hydrogen showing a maximum quality of about 0.05. In a separate, but related study, the authors report that although the Martinelli parameter was successful in correlating heat transfer data, it was not at all successful in correlating the pressure drop data which they obtained from this long helical tube. Instead, they found that the use of a homogeneous model described the pressure drop data reasonably well.

VI. HELIUM I, REGION 3

Since Region 3 is devoted entirely to the single-phase fluid where a good deal of heat transfer work has been done for other fluids, one might expect less difficulty in extending the conventional correlations to the helium case. It may be, however, that the extreme property differences for helium and the property behavior for liquid helium, particularly, would make the helium behavior significantly different from the conventional fluids. For conventional fluids the Dittus-Boelter⁵⁵ correlation to produce the Nusselt number as

$$Nu = 0.023 (Re)^{0.8} (Pr)^{0.4} ,$$

is generally satisfactory. The only experimental work for helium reported in Region 3 is that of Dorey.⁶⁰ Dorey employed a test section of a small flat plate and investigated the cases of both free and forced convection. In cases of both free and forced convection, Dorey's experimental data were obtained at Reynolds numbers which were in the general transition region between laminar and turbulent flow. He compared his data with respect to both the laminar and turbulent heat transfer predictions of the conventional correlations. For the free convection case, a difference between the analytical expression for the two flow regimes is expressed in the power (a) to which the product of the Grashof and Prandtl number is raised in the following expression:

$$Nu = (\text{const})(Gr \cdot Pr)^{(a)} .$$

Although the constant coefficient in the expression varies between the two flow regimes, the exponent (a) is a better indicator of the flow regime. In this transition region for free convection, Dorey found that the exponent conventionally used for the turbulent case more nearly described his experimental data. He recommended the following expression for the heat transfer coefficient for free convection for helium in the Reynolds number range which is transition between laminar and turbulent flow:

$$h = 0.16 \left(\frac{P_l^2 k_l g \beta C_p (T_w - T_b)}{\mu_l} \right)^{1/3} . \quad (12)$$

For forced convection, Dorey investigated two equations for laminar and turbulent flow. These expressions were recommended by Jacob⁶¹ for flat-plate flow rather than the more conventional case of flow inside tubes considered previously. These two expressions are

$$Nu = 0.664 Re^{0.5} Pr^{0.5} \quad (\text{laminar}) \quad (13)$$

$$Nu = 0.36 Re^{0.8} Pr \quad (\text{turbulent}) . \quad (14)$$

Again as shown in Fig. 24, Dorey's data in a transition region between the two flow modes fell between predictions of the analytical exponents of the two modes.

Brechna²⁵ has reported some forced convection, liquid helium data discussed previously in Region 1. He finds that the coefficient in the conventional turbulent, forced convection equation is increased by a factor of about 1.7 for the case of helium heat transfer. It is not clear at this time whether the data of Brechna were obtained for Region 1 or Region 3; however, it is presumed that some of these data were obtained in Region 3.

VII. REGION 4

A full discussion of helium heat transfer in Region 4 is not considered in this paper. There are two reasons for this. First, helium in this region would not be expected to behave differently than another gas. Some small modifications might be required by the rather significant properties differences, particularly that of viscosity; however, the author is not aware of any investigators who have reported the need for such modifications. Most of the helium gas studies, however, have been carried out at considerably higher temperature than those shown or considered in this paper. The second reason for omission of the Region 4 is that for the most part the temperatures in Region 4 are presumed to be too high for cooling superconductors.

VIII. SUMMARY AND RECOMMENDATIONS

VIII.1. Region 1 - Supercritical Near Transposed Critical

- a) This region should be avoided, if at all possible, if oscillations in pressure and temperature are undesirable.
- b) The region boundary appears to be generally defined by the transposed critical line and the minimum constant pressure line which does not exhibit the "hump" or rapidly changing property behavior similar to that at the critical point. This pressure is at about 15 atm.
- c) The conventional heat transfer correlation using constant properties,

$$\text{Nu} = 0.023 (\text{Re})^{0.8} (\text{Pr})^{0.4} , \quad (15)$$

can probably be used as a general guide to predict the heat flux for forced convection, turbulent heat transfer inside conduits. Enhancement is theoretically possible but, since heat transfer behavior is unknown and property values are uncertain, one should not expect to obtain enhancement unless a development program is undertaken. Degradation is perhaps more likely for systems in this region.

- d) Heat transfer and property data are urgently needed in this region. First studies should be to:
 - i) Define the region boundaries.
 - ii) Establish the magnitude and nature of the oscillations in the region.
 - iii) Investigate arrangements to minimize the oscillations.
 - iv) Establish a heat transfer predictive system better than a constant property correlation.

VIII.2. Region 2 - Boiling, Two Phase

VIII.2.1. Pool boiling

- a) For pool boiling, it would appear that the correlations for conventional fluids can be used with approximately the same degree of reliability as for other cryogenic liquids.

Nucleate - Kutateladze,²⁷ Eq. (3).

Maximum nucleate - Kutateladze,²⁷ Zuber et al.,³⁴ Eq. (4).

Film - Breen and Westwater,²⁹ Eq. (5).

Minimum film - Lienhard and Wong,³¹ Eq. (6).

b) These correlations do not consider some of the significant variables and should be used with caution. Among these variables which seem to have a more pronounced influence with helium are:

i) Hysteresis - Lyon,⁵³ Cummings and Smith,⁴⁰ Thibault et al.⁶²

ii) Geometry effects - Lyon,⁵³ Sydoriak and Roberts.⁵¹

iii) Substrate effects - Cummings and Smith.⁴⁰

c) Other variables, not accounted for in the correlations, but which have been shown to have a significant influence with other cryogenic liquids are:

i) Surface roughness - Boissin et al.,⁵⁴ Cummings and Smith.⁴⁰

ii) Surface chemistry - Lyon.⁴³

iii) Pressure effects for the nucleate boiling curve are reasonably well accounted for by the nucleate correlations for

$$p/p_{\text{crit}} < 0.6.$$

For pressures above this value the correlations do not appear to be reliable.

iv) Subcooling effects are unknown (see Fig. 21 for estimates).

VIII.2.2. Forced convection boiling

For forced convection boiling, the single reported work, de La Harpe et al.⁵⁸ indicated behavior similar to conventional fluids. The nucleate boiling or wetted surface region appears to be extended in quality.

VIII.2.3. Recommendations for further work

Further work in this region appears to be less critically needed than in the other areas. Perhaps the regions of surface and substrate effects, geometry effects, pressure effects and forced convection should have first priority for future investigations.

VIII.3. Regions 3 and 4

a) The very limited data of Brechna,²⁵ and Dorey,⁶⁰ indicate the use of conventional correlations, Eqs. (12), (13), (14), and (15) may be conservative.

b) Fluid property data would indicate that the conventional correlations can be used with reasonable confidence except, perhaps, for liquid helium at lower pressures where the transport properties have the opposite slope of that for other liquids.

c) Some further work is rather urgently needed, however, to establish more positively whether or not conventional correlations may be used without modification.

NOMENCLATURE

Latin Letters

a	= Empirically determined exponent.
C_p	= Specific heat capacity at constant pressure.
D	= Diameter.
F_{sub}	= Multiplying factor for peak heat flux due to subcooling $(q/A)_{sub} = (q/A)_{sat} F_{sub}$.
h	= Convective heat transfer coefficient.
h'_{fg}	= "Effective" latent heat vaporization, defined by Eq. (5).
h_{fg}	= Latent heat of vaporization at saturation.
g	= Acceleration of gravity.
Gr	= Grashof's number, $\rho g \beta (T_w - T_b) y^3 / \mu^2$, dimensionless.
k	= Thermal conductivity.
Nu	= Nusselt number, (hD/k)
Nu_{calc}	= Calculated Nusselt number, dimensionless.
P	= Pressure.
Pr	= Prandtl number, $(c\mu/k)$.
q/A	= Rate of heat transfer per unit area.
Re	= Reynolds number, $(uD\rho/\mu)$.
T	= Temperature.
u	= Average fluid velocity.
x	= Quality, (mass vapor/mass mixture), dimensionless.
y	= Length dimension.

Greek Letters

β	= Thermal coefficient of volumetric expansion.
ϵ_h	= Eddy diffusivity of energy.
μ	= Newtonian coefficient of viscosity.
ρ	= Density
ν	= Kinematic viscosity.
σ	= Surface tension between the liquid and its own vapor.
X_{tt}	= Martinelli parameter, dimensionless.

Subscripts

b	= Indicates bulk property.
l	= Subscripted liquid property.
w	= Wall or solid surface conditions.
x	= Proportional location in thermal boundary layer to establish temperature for property evaluation.

sat = Saturated conditions.
v = Vapor or gas condition.
c = Critical condition.
tp = Two phase.

REFERENCES

1. R.J. Corruccini, in Liquid Hydrogen (Inst. Intern. Froid, Paris, 1965), p. 65.
2. H.J.M. Hanley and G.E. Childs, to be published.
3. O.V. Lounasmaa, D. Phil. thesis, Oxford University (1958).
4. H.H. Kolm, M.J. Leupold, and R.D. Hay, in Advances in Cryogenic Engineering (Plenum Press, 1966), Vol. 11, p. 530.
5. N.L. Dickinson and C.P. Welch, Trans. ASME 80, 746 (1958).
6. E.N. Dubrovina and V.P. Skripov, in Proc. 2nd All-Soviet Union Conference on Heat and Mass Transfer, Vol. I (translation by Rand Corp., R-451-PR) (1966).
7. J.D. Griffith and R.H. Sabersky, Am. Rocket Soc. Journal, 289 (1960).
8. R.C. Hendricks, R.W. Graham, Y.Y. Hsu, and R. Friedman, National Aeronautics and Space Administration Technical Note NASA TN D-3095 (1966).
9. R.S. Thurston, J.D. Rogers, and V.J. Skoglund, in Advances in Cryogenic Engineering (Plenum Press, 1966), Vol. 12, p. 438.
10. R.S. Thurston, in Advances in Cryogenic Engineering (Plenum Press, 1965), Vol. 10, p. 305.
11. R.S. Thurston, Los Alamos Scientific Laboratory Report LA-3616 (1966).
12. A.J. Cornelius, Argonne National Laboratory Report ANL-7032 (1965).
13. R.D. Wood and J.M. Smith, A. I. Ch. E. J. 10, 180 (1964).
14. D.B. Spalding, J. Appl. Mech. 28, 455 (1961).
15. R.G. Deissler, Trans. ASME 76, 73 (1954).
16. R.G. Deissler, J. Heat Transfer, Trans. ASME 82C, 160 (1960).
17. R.C. Hendricks, R.W. Graham, Y.Y. Hsu, and A.A. Medeiros, Am. Rocket Soc. Journal 244 (1962).
18. R.C. Martinelli and D.B. Nelson, Trans. ASME 70, 695 (1948).
19. R.P. Bringer and J.M. Smith, A. I. Ch. E. J. 3, 49 (1957).
20. W.S. Miller, J.D. Seader, and D.M. Trebes, in Pure and Applied Cryogenics (Pergamon Press, 1966), Vol. 4, p. 173.
21. W.S. Miller, presented at Am. Inst. Astronaut. Aeron. 2nd Propulsion Joint Specialist Conference, Colorado Springs, Colo., 1966, Paper No. 66-580.
22. R.G. Deissler and A.F. Presler, in International Developments in Heat Transfer (ASME, 1963), p. 579.

23. H.L. Hess and H.R. Kunz, J. Heat Transfer, Trans. ASME 87C, 41 (1965).
24. G. Klipping and K. Kutzner, in Pure and Applied Cryogenics (Pergamon Press, 1967), Vol. 6, p. 97.
25. H. Brechna, Stanford Linear Accelerator Center Report SLAC-PUB-274 (1967).
26. E.G. Brentari and R.V. Smith, in International Advances in Cryogenic Engineering (Plenum Press, 1965), Vol. 10, p. 325.
27. S.S. Kutateladze, State Sci. and Tech. Pub. of Lit. on Machinery, Moscow (Atomic Energy Commission Translation 3770, Tech. Info. Service, Oak Ridge, Tennessee).
28. N. Zuber, U.S. Atomic Energy Commission Report AECU-4439 (AEC, Oak Ridge, Tennessee, 1959).
29. B.P. Breen and J.W. Westwater, Chem. Eng. Progr. 58, No. 7, 67 (1962).
30. L.A. Bromley, Chem. Eng. Progr. 46, No. 5, 221 (1950).
31. J.H. Lienhard and P.T.Y. Wong, J. Heat Transfer, Trans. ASME 86C, 220 (1964).
32. W.R. Gambill, Brit. Chem. Engr. 8, No. 2, 93 (1963).
33. H.J. Ivey and D.J. Morris, AEEW-R137 (1962).
34. N. Zuber, M. Tribus, and J.W. Westwater, in International Developments in Heat Transfer (ASME, 1963), p. 230.
35. R.W. Graham, R.C. Hendricks, and R.C. Ehlers, in International Advances in Cryogenic Engineering (Plenum Press, 1965), Vol. 10, p. 342. Also: National Aeronautics and Space Administration Technical Note NASA TN D-1883 (1965).
36. G.C. Vliet and G. Leppert, J. Heat Transfer, Trans. ASME 86C, 59 (1964).
37. R.C. Hendricks and R.R. Sharp, National Aeronautics and Space Administration Technical Note NASA TN D-3095 (1964).
38. F.D. Moore and R.B. Mesler, A. I. Ch. E. J. 7, 620 (1961).
39. R.R. Sharp, National Aeronautics and Space Administration Technical Note NASA TN D-1997 (1964).
40. R.D. Cummings and J.L. Smith, Jr., in Pure and Applied Cryogenics (Pergamon Press, 1967), p. 85.
41. H.F. Bowman, Ph.D. thesis, Massachusetts Institute of Technology (1968).
42. N.R. Mikhail, Ph.D. thesis, Imperial College of Science and Technology, London (1952).
43. D.N. Lyon, Intern. J. Heat and Mass Transfer 7, No. 10, 1097 (1964).
44. C.R. Class, J.R. DeHaan, M. Piccone, and R.B. Cost, in Advances in Cryogenic Engineering (Plenum Press, 1960), Vol. 5, p. 254.
45. G. Tuck, General Dynamics/Astronautics Report No. 55D, 859 (1962).
46. R.J. Good and G.V. Ferry, in Advances in Cryogenic Engineering (Plenum Press, 1963), Vol. 8, p. 306.
47. W.M. Rohsenow, Trans. ASME 74, 969 (1952).
48. R.K. Young and R.L. Hummel, presented at A. I. Ch. E. Meeting, Boston, Mass. (1964).
49. C.P. Costello, C.O. Buck, and C.C. Nichols, Heat Transfer Conference, Cleveland, Ohio (A. I. Ch. E., 1964).
50. S.G. Bankoff, A. I. Ch. E. J. 4, 24 (1958).

51. S.G. Sydoriak and T.R. Roberts, in Pure and Applied Cryogenics (Pergamon Press, 1966), Vol. 6, p. 115.
52. M.N. Wilson, *ibid.*, p. 109.
53. D.N. Lyon, in International Advances in Cryogenic Engineering (Plenum Press, 1965), Vol. 10, p. 371.
54. J.C. Boissin, J.J. Thibault, J. Roussel, and E. Faddi, in Advances in Cryogenic Engineering (Plenum Press, 1968), Vol. 13, p. 607.
55. F.W. Dittus and L.M.K. Boelter, Univ. Calif. (Berkeley) Publ. Eng. 2, 443 (1930).
56. E.G. Brentari, P.J. Giarratano, and R.V. Smith, National Bureau of Standards Technical Note No. 317 (1965).
57. P.J. Giarratano and R.V. Smith, in Advances in Cryogenic Engineering (Plenum Press, 1966), Vol. 11, p. 492.
58. A. de La Harpe, S. Lehongre, J. Mallard, and C. Johannes, presented at Cryogenic Engineering Conference, Cleveland, Ohio, 1968.
59. C.C. Wright and H.H. Walters, Wright Air Development Center Technical Report WADC 59-423 (1959). Also: H.H. Walters, in Advances in Cryogenic Engineering (Plenum Press, 1961), Vol. 6, p. 509.
60. A.P. Dorey, Cryogenics 5, 146 (1965).
61. M. Jacob, Heat Transfer (Wiley, 1949).
62. J.J. Thibault, J. Roussel, and E. Faddi, in Pure and Applied Cryogenics (Pergamon Press, 1966), Vol. 4, p. 249.

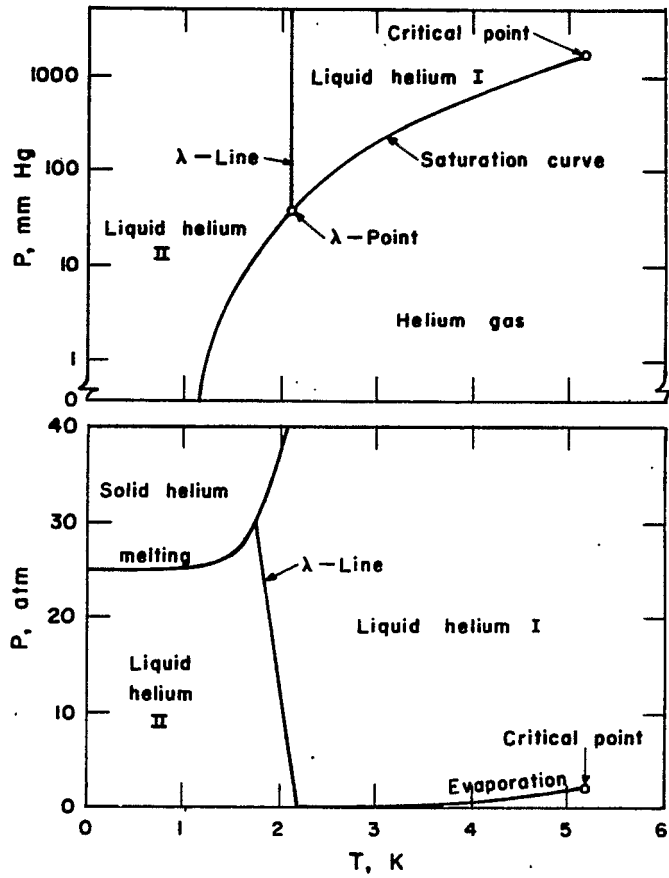


Fig. 1. Pressure-temperature diagrams for helium.

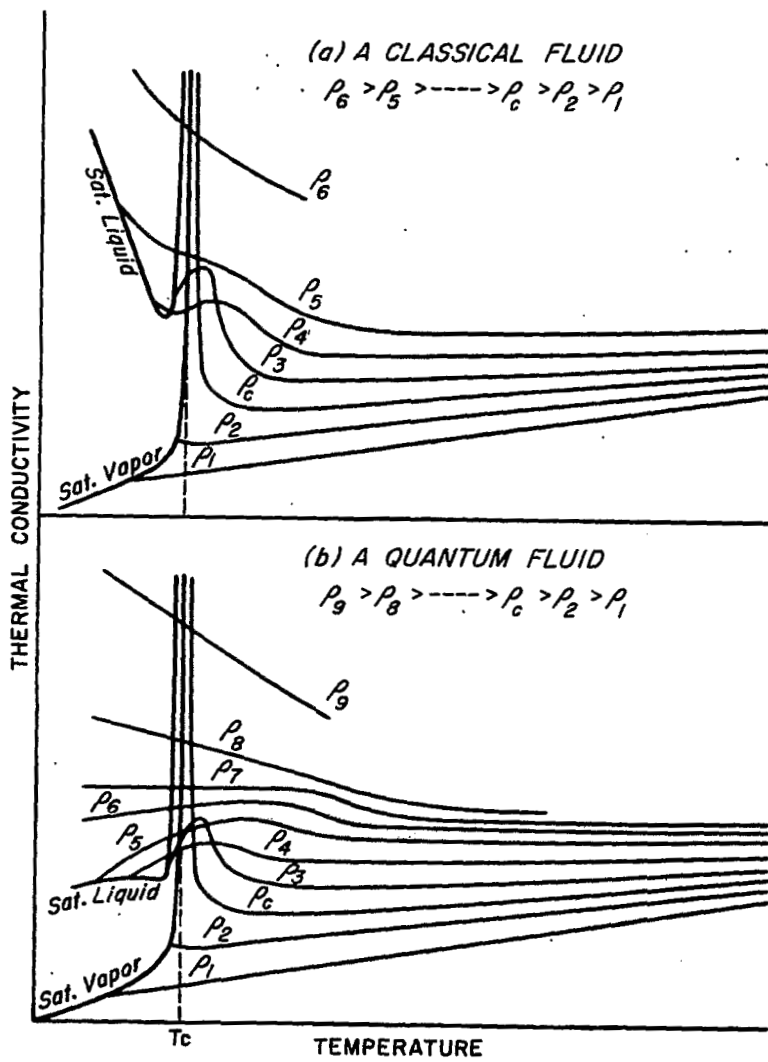


Fig. 2. Comparison of the behavior of thermal conductivity for a classical and for a quantum fluid from Corruccini (Ref. 1).

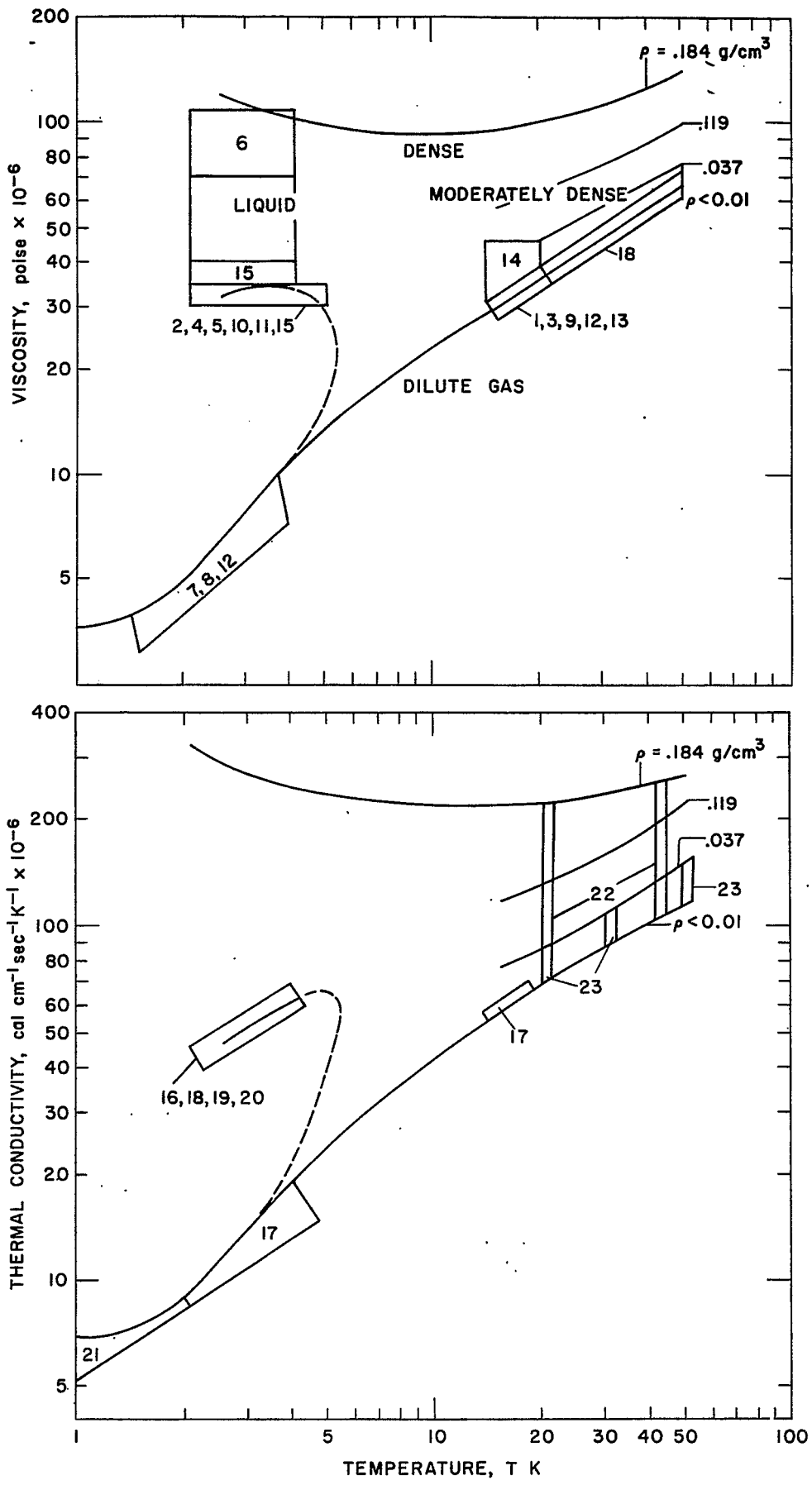


Fig. 3. Viscosity and thermal conductivity diagrams for helium showing regions of reported experimental data from Hanley and Childs (Ref. 2). Lines are for conditions of constant density.

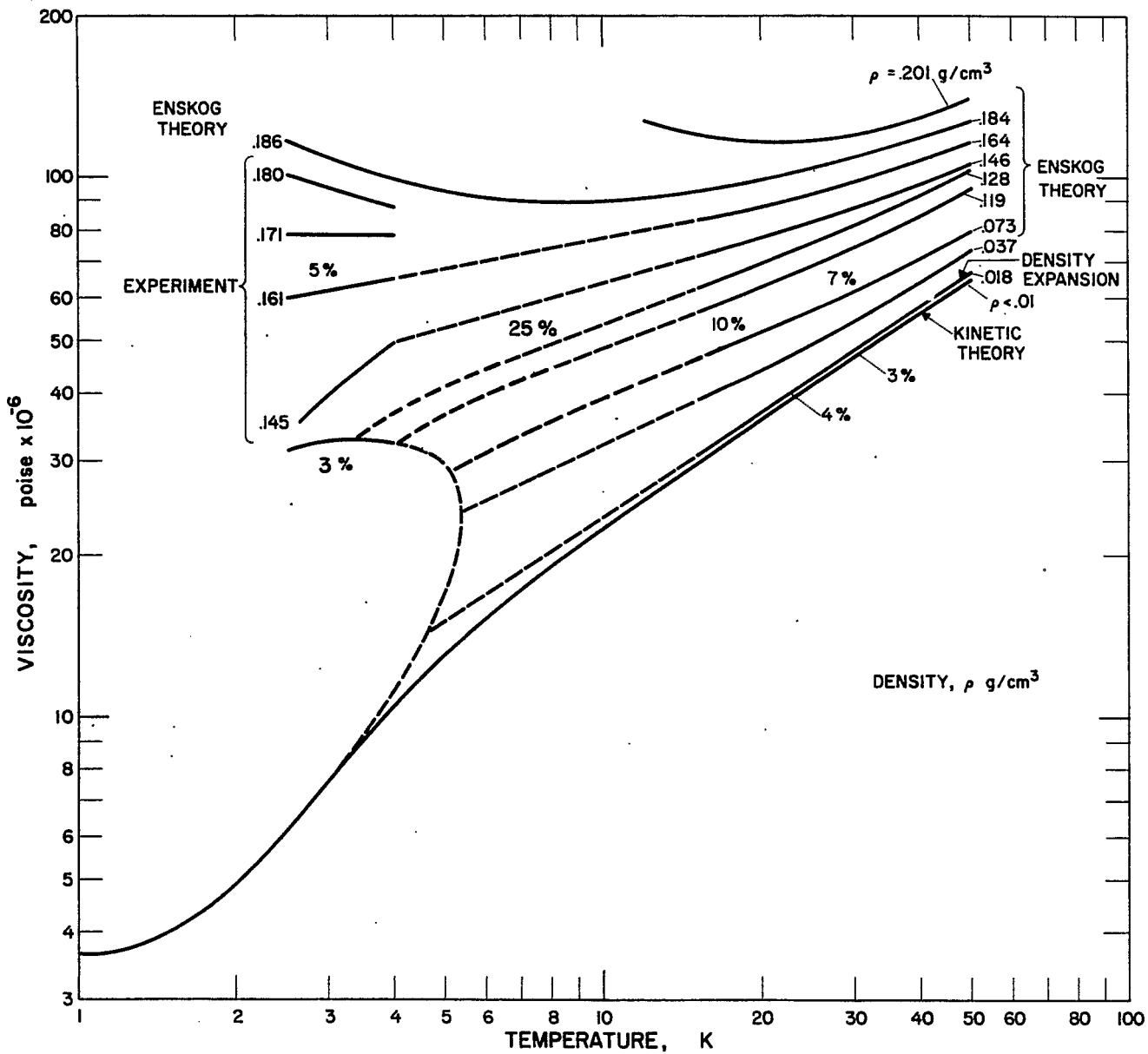


Fig. 4. The viscosity of helium at constant density. Solid lines represent data from theory or experiment which have the approximate reliability shown. Dashed lines indicate regions where there are no reliable data. From Hanley and Childs (Ref. 2).

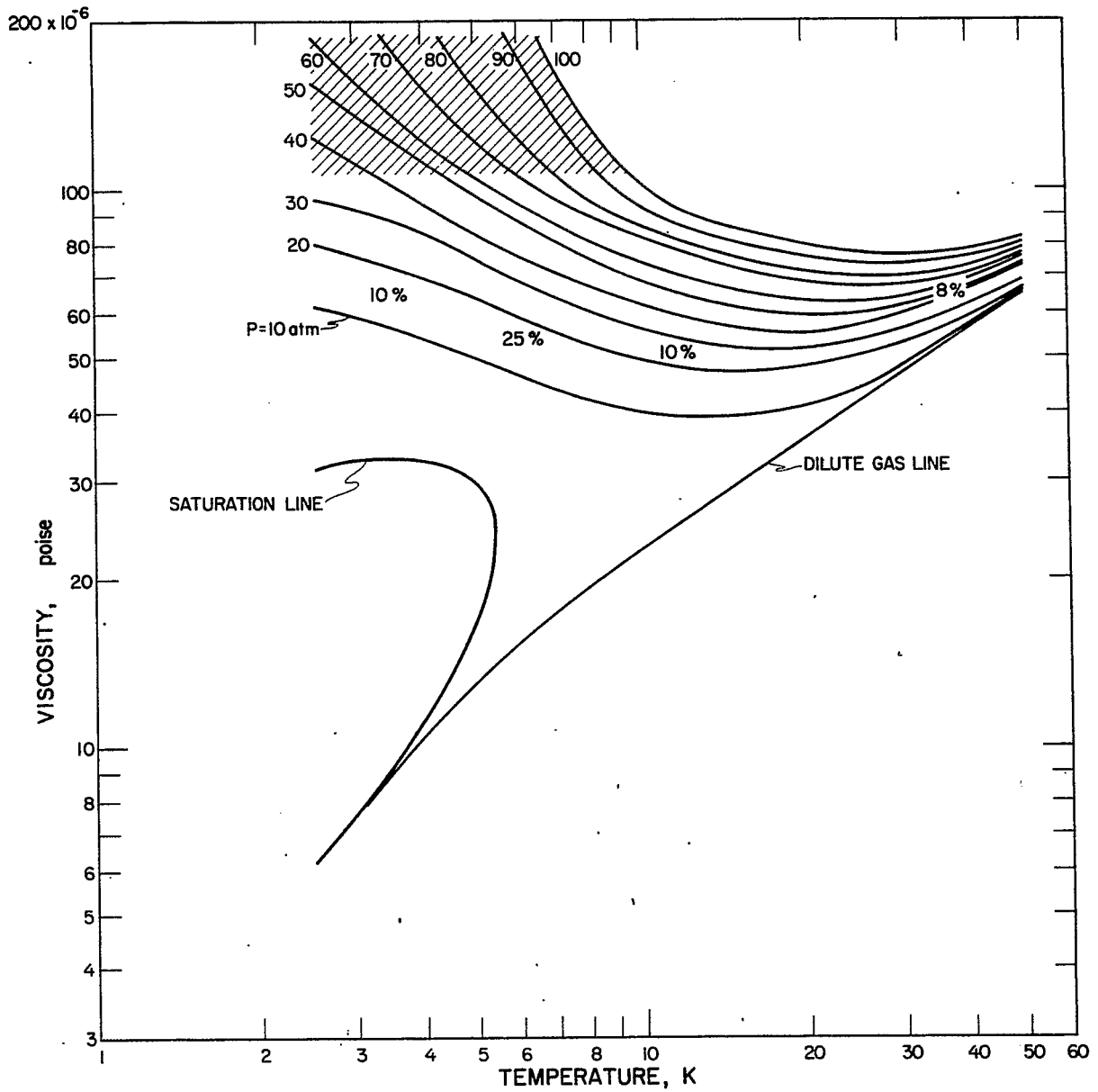


Fig. 4a. Viscosity of helium at constant pressure. Data are from Fig. 4. Conversion was made by use of properties in NBS TN 154 by D.B. Mann (1962). Crosshatched area indicates regions where data are considered unreliable.

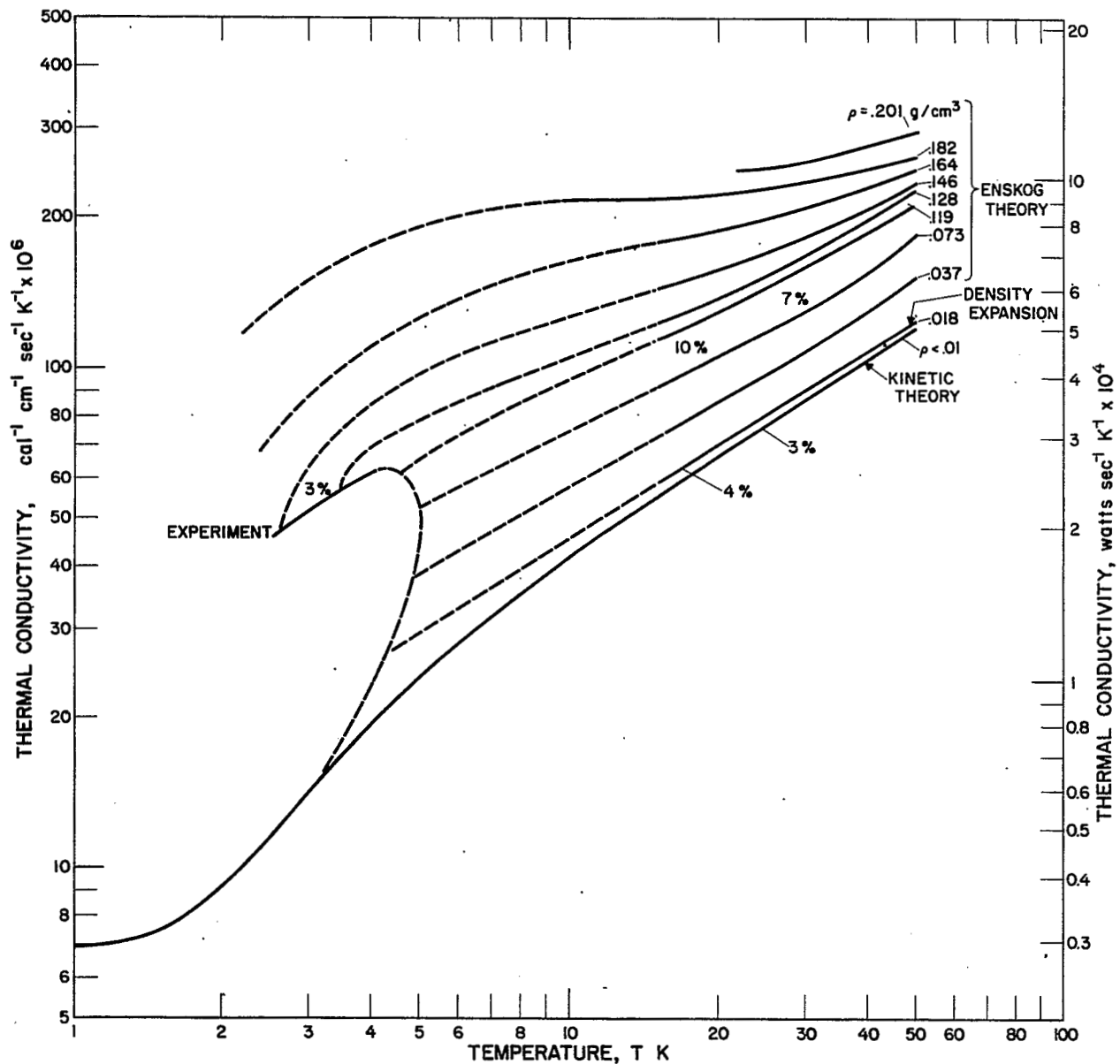


Fig. 5. The thermal conductivity of helium at constant density. Solid lines represent data from theory or experiment which have the approximate reliability shown. From Hanley and Childs (Ref. 2).

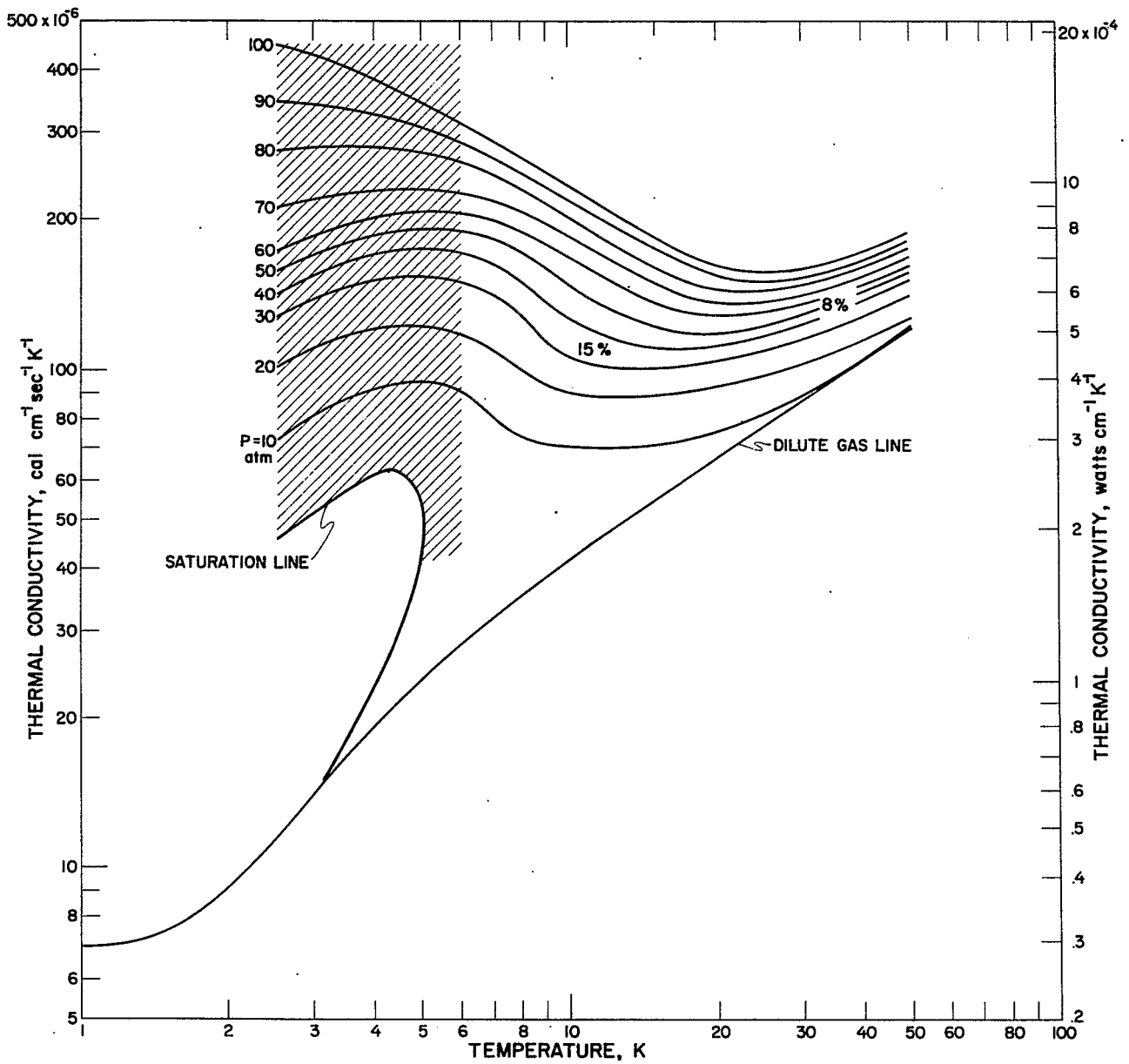


Fig. 5a. Thermal conductivity of helium at constant pressure. Data are from Fig. 5. Conversion was made by use of properties in NBS TN 154 by D.B. Mann (1962). Crosshatched area indicates regions where data are considered unreliable.

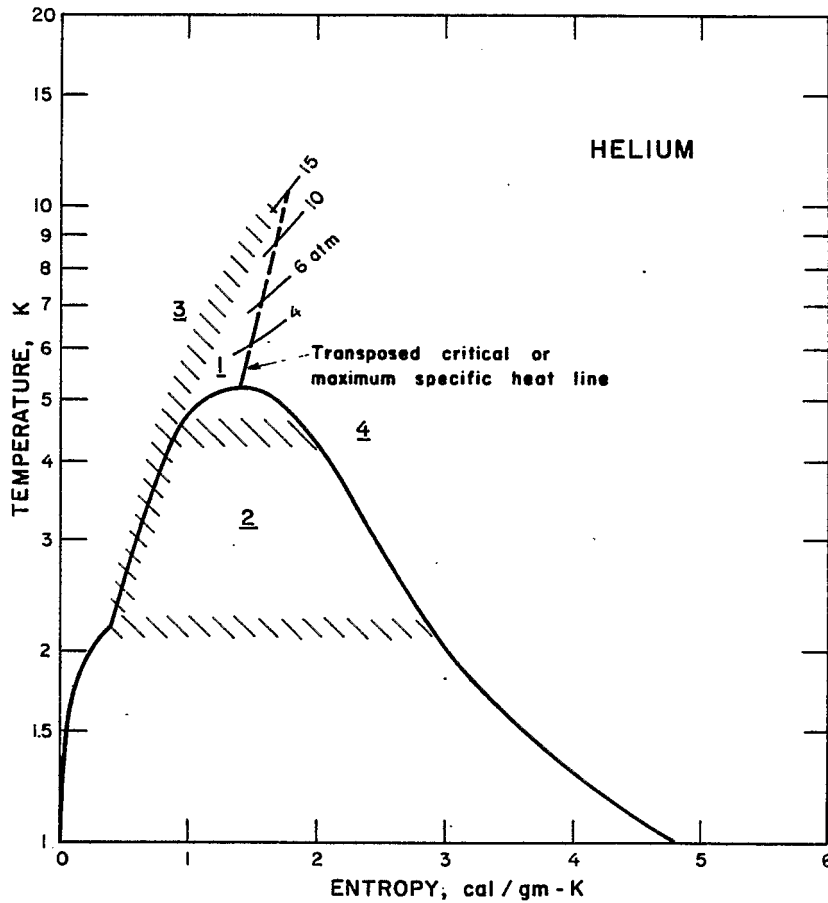
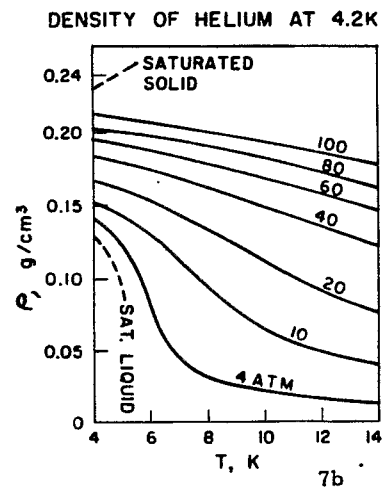
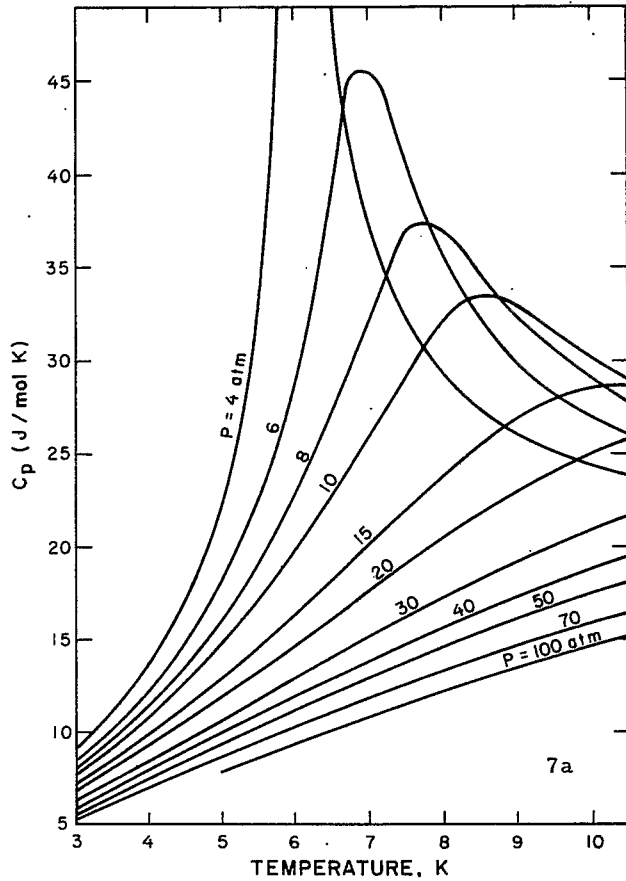


Fig. 6. Temperature-entropy diagram for helium showing the regions of similar property and heat transfer behavior.



Figs. 7a & 7b. Specific heat data from Lounasmaa (Ref. 3) and density from Kolm et al. (Ref. 4) for helium showing the large property changes with temperature in the region of the critical and the transposed critical.

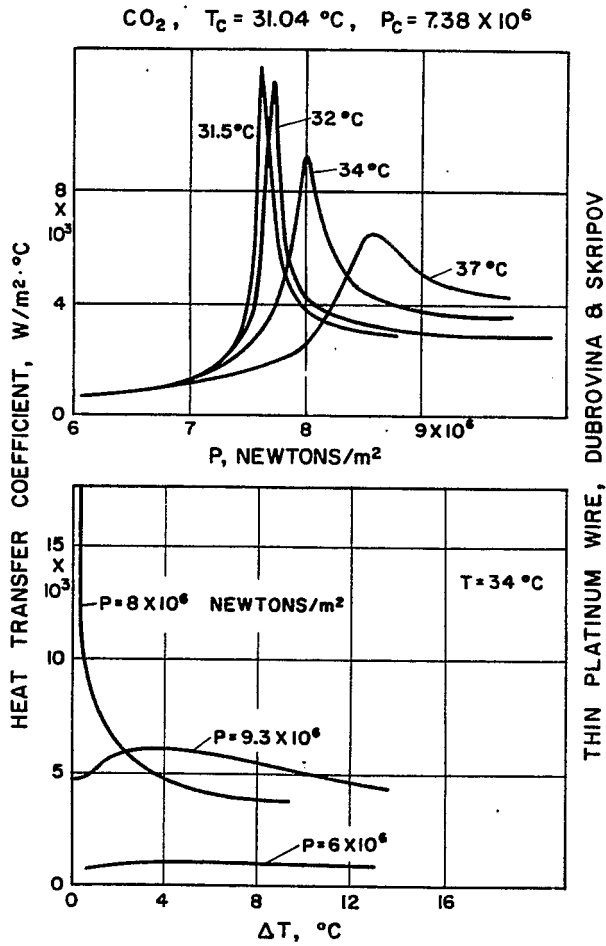


Fig. 8. Heat transfer coefficients from Dubrovina and Skripov (Ref. 6). Data show the coefficient behaves as the properties near the critical or transposed critical if the temperature differences are very small.

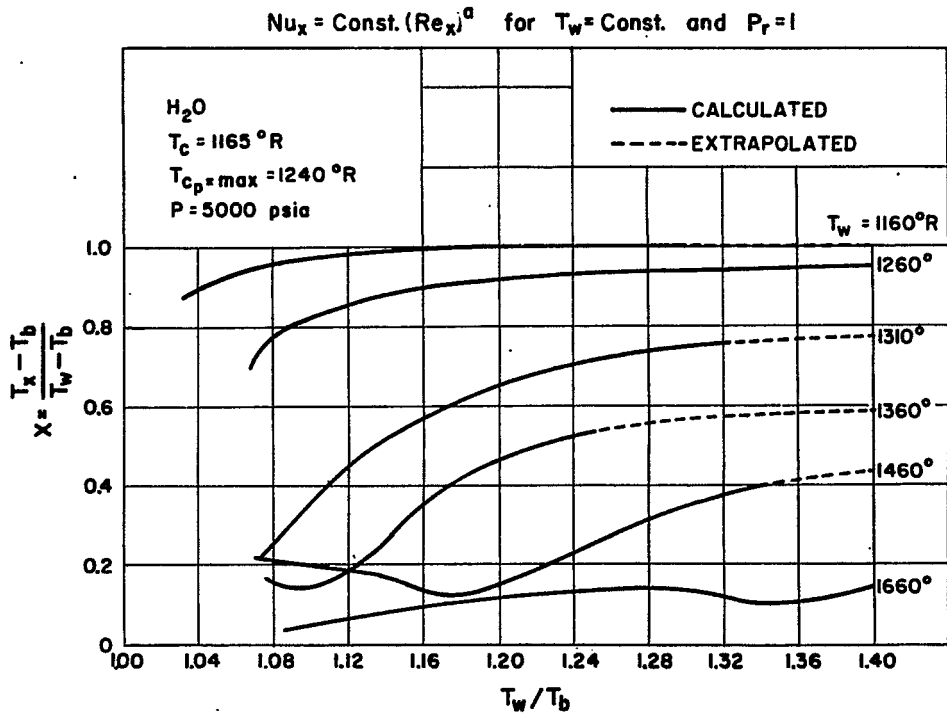


Fig. 9. Diagram showing reference temperature locations for property evaluation in the Nusselt and Reynolds numbers relationship. From Deissler (Ref. 15).

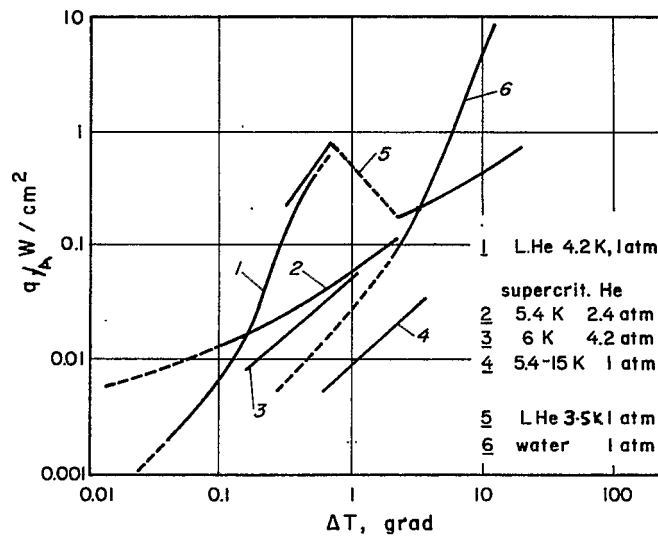


Fig. 10. Heat transfer to supercritical helium, boiling helium and boiling water at 1 atm. From Klipping and Kutzner (Ref. 24).

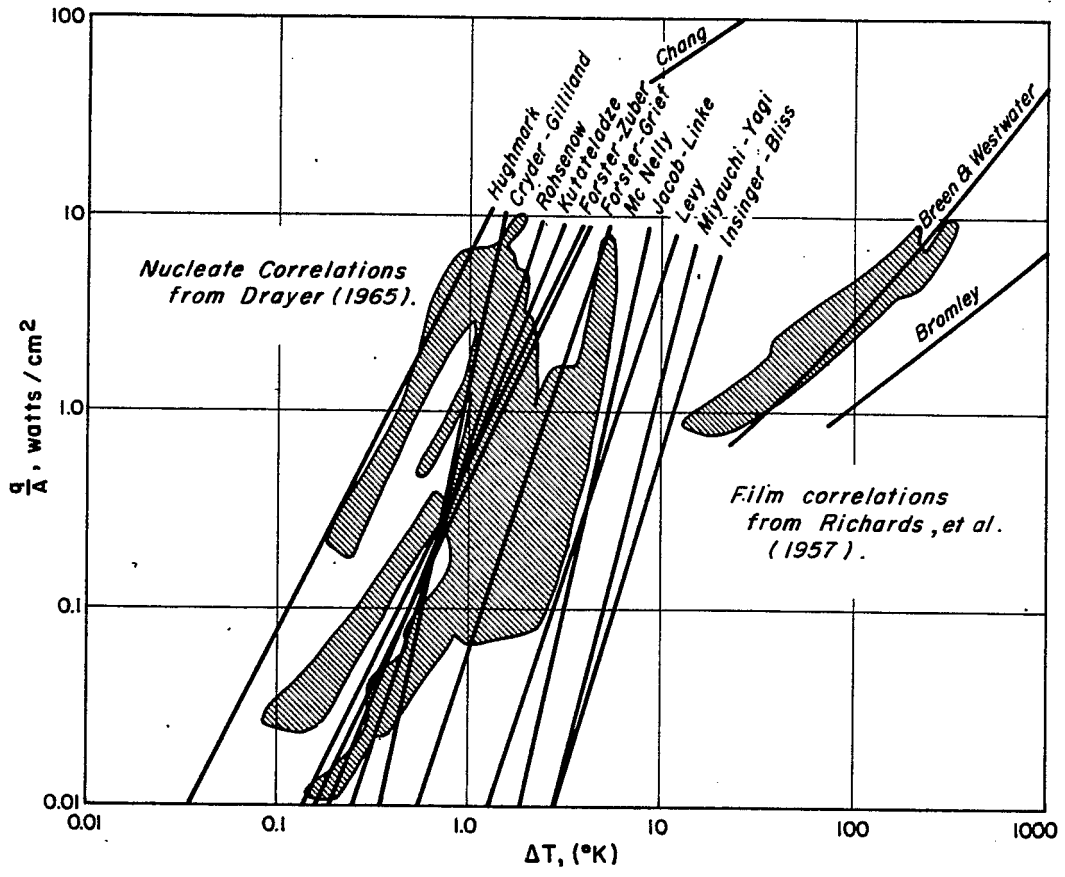


Fig. 11. Comparison of various boiling heat transfer correlations from the literature for hydrogen at 1 atm pressure with the reported experimental data shown as crosshatched areas. From Brentari et al. (Ref. 56).

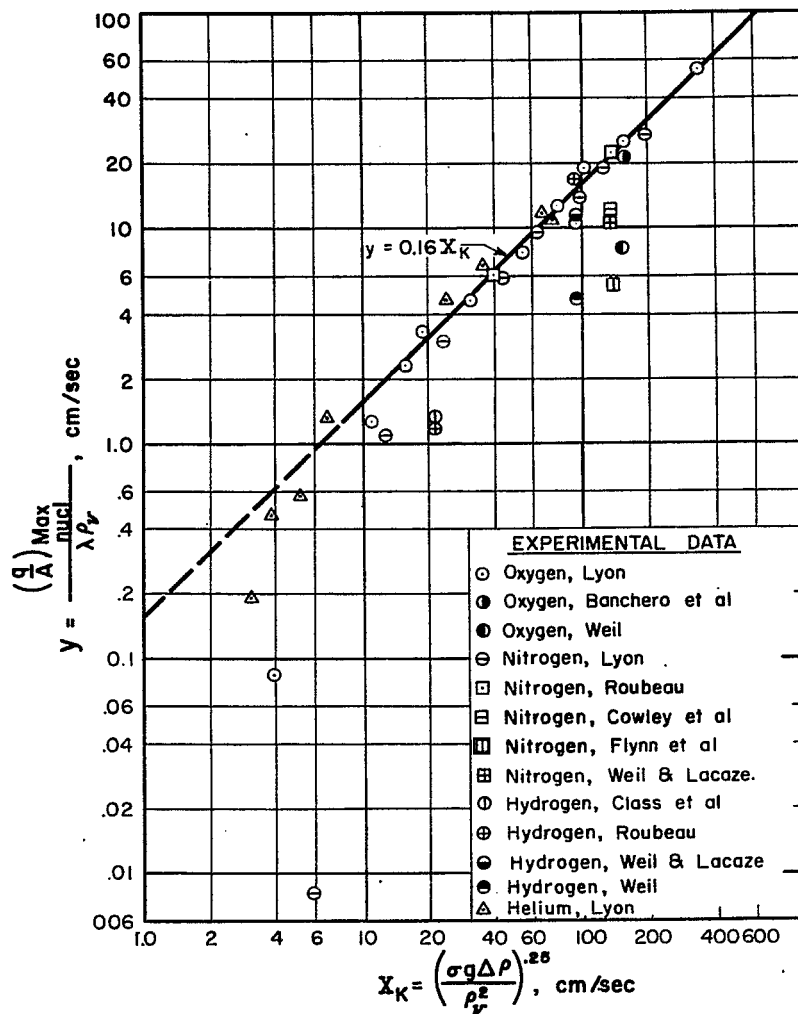


Fig. 12. Comparison of the experimental maximum nucleate heat transfer fluxes for cryogenic liquids with the Kutateladze maximum correlation. From Brentari et al. (Ref. 56).

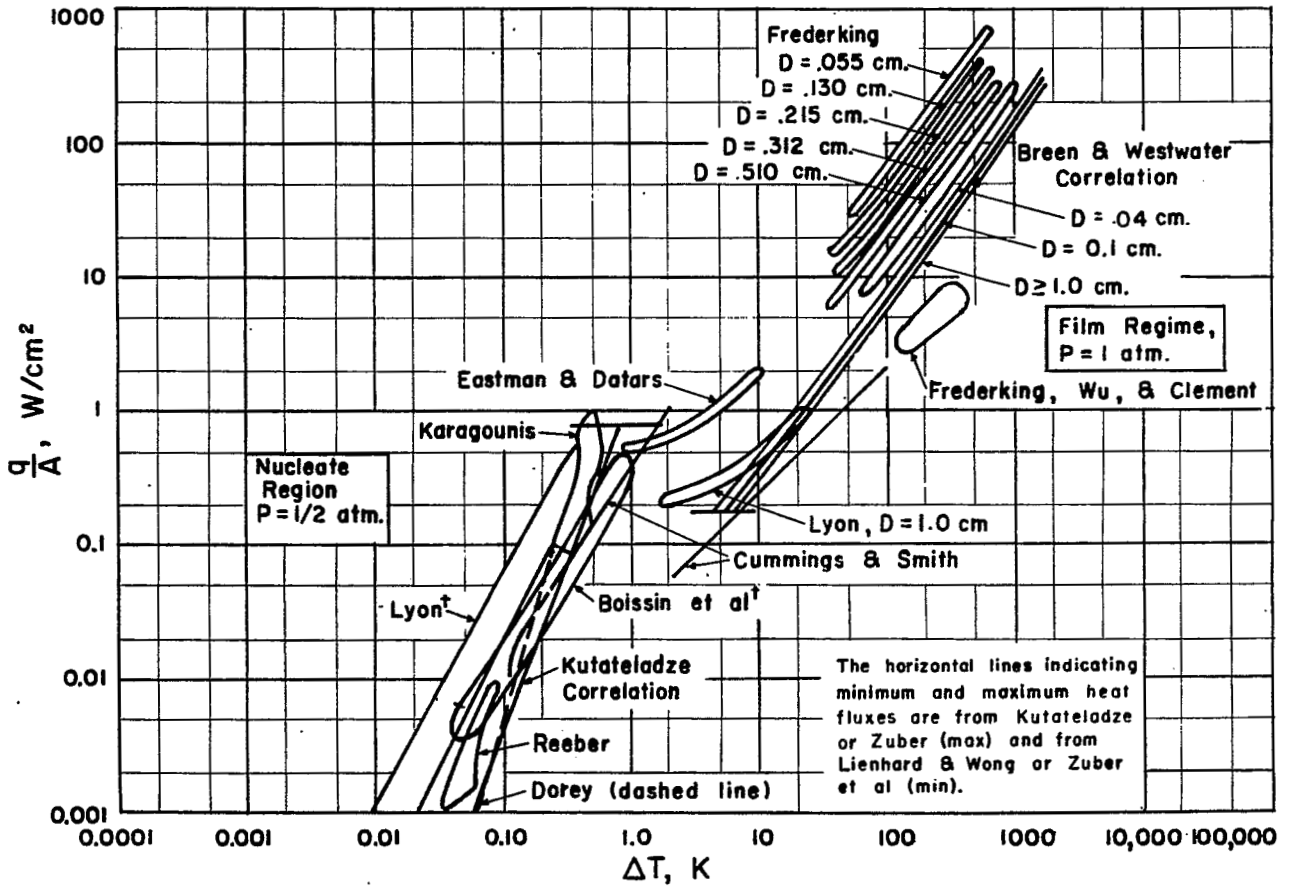


Fig. 13. Pool boiling of helium compared with results from correlations. Data identified by † has been corrected to values for the $\frac{1}{2}$ atm case by use of the pressure dependence implied from the Kutateladze correlation.

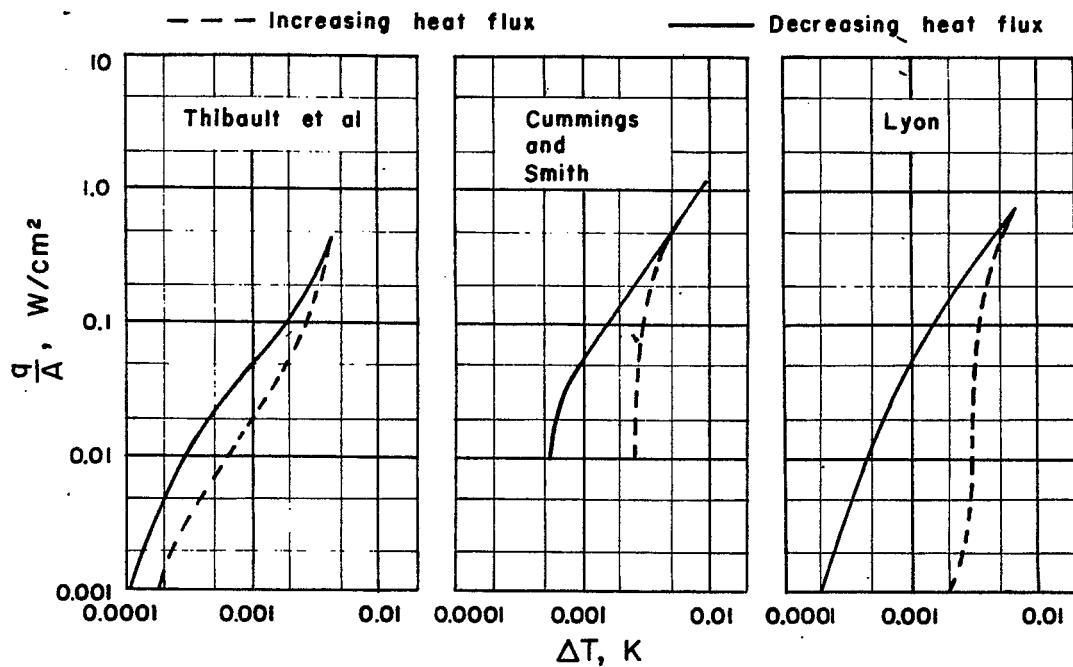


Fig. 14. Hysteresis or the effect of delayed bubble inception in the nucleate boiling region for helium as reported by three investigators.

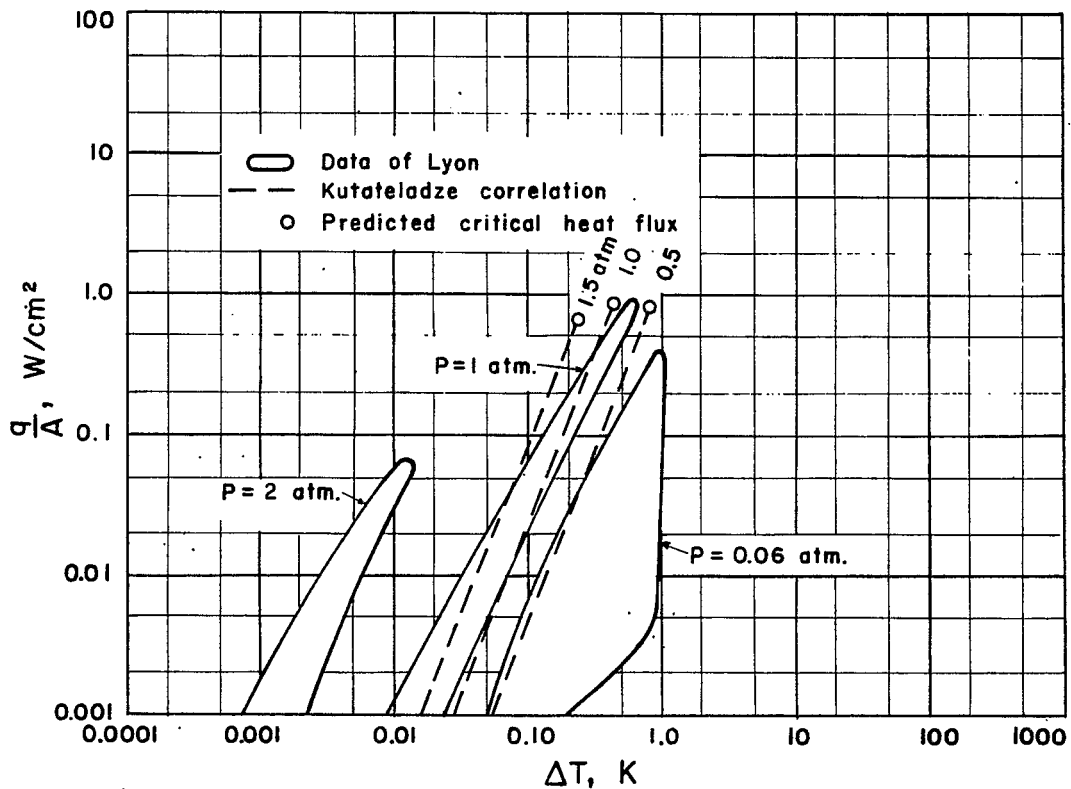


Fig. 15. Predicted nucleate boiling results from the Kutateladze correlation compared with experimental data from Lyon (Ref. 53) to show the reliability of the correlation at different pressure levels.

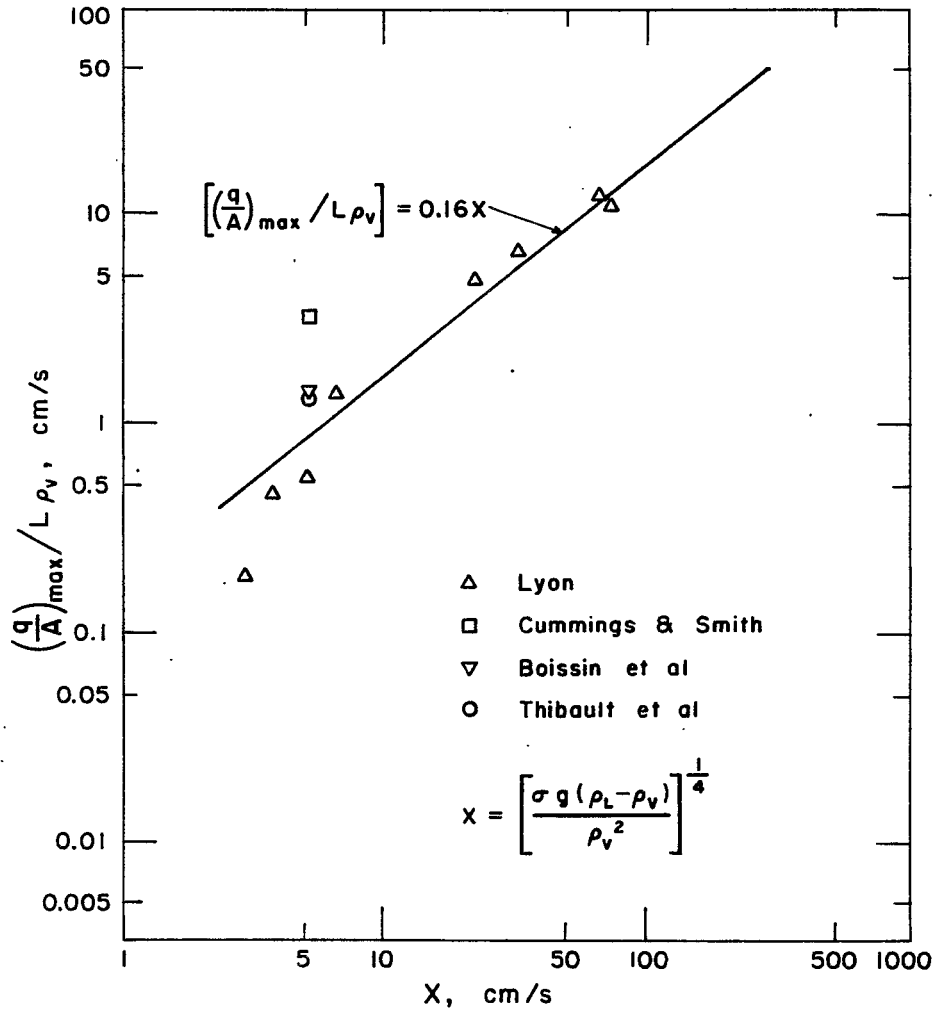


Fig. 16. Experimental data of maximum nucleate boiling fluxes compared with predictive results from the Kutateladze or Zuber correlation (Refs. 27 and 28).

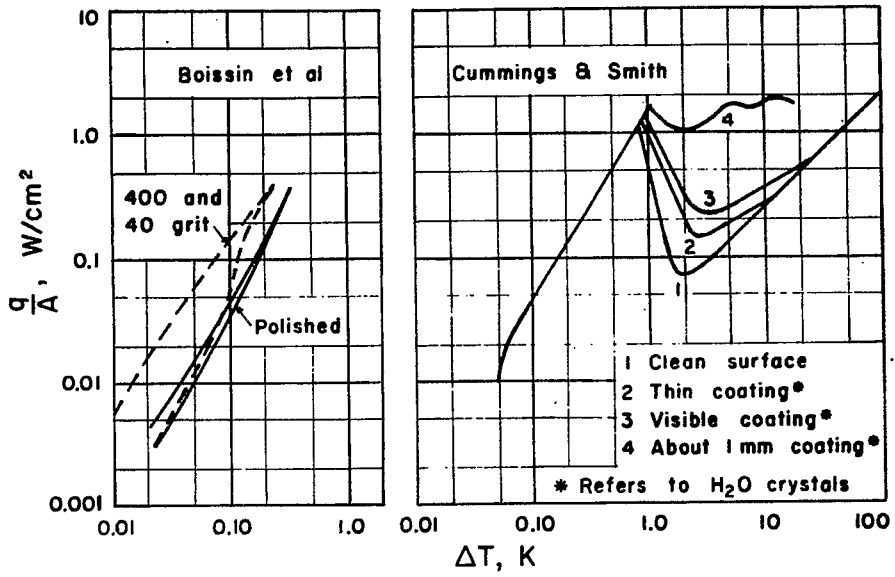


Fig. 17. Surface roughness effects for pool boiling with helium as reported by two investigators.

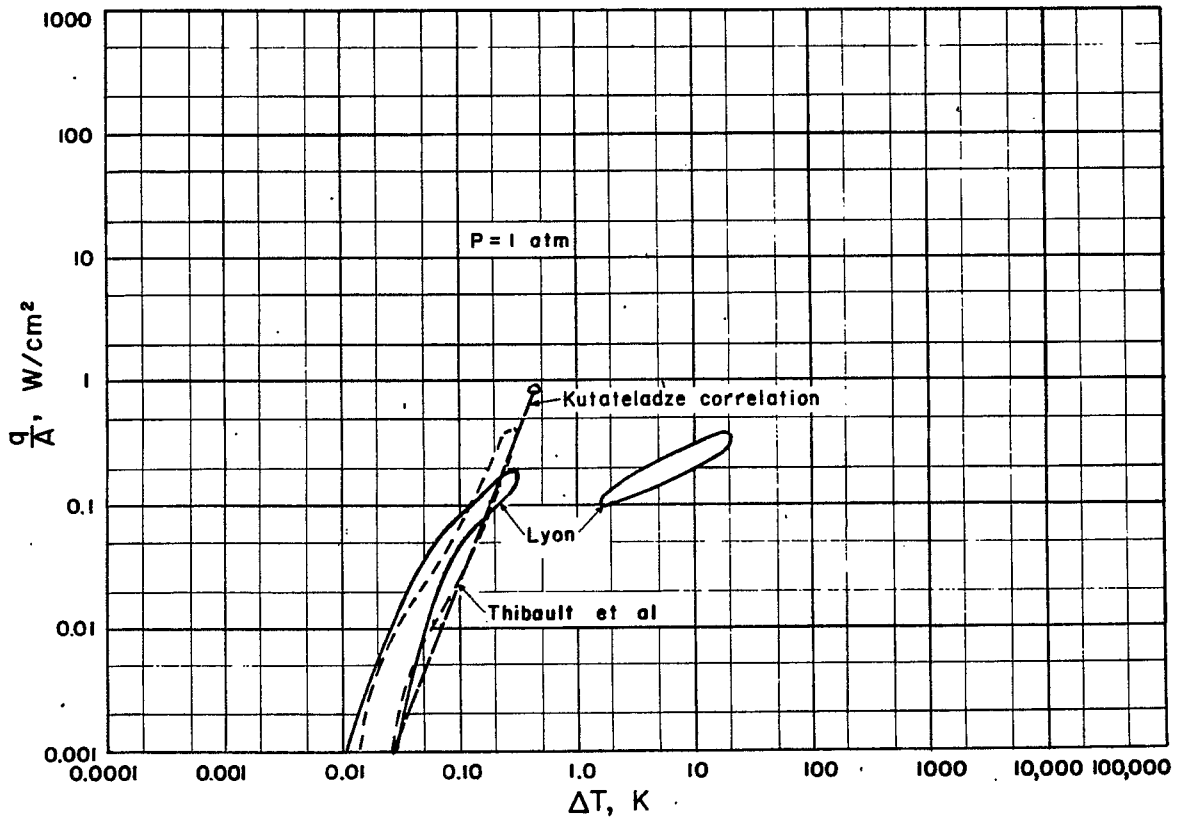


Fig. 18. Pool, nucleate boiling of helium from heated surfaces facing downward. Circle indicates predicted burnout condition.

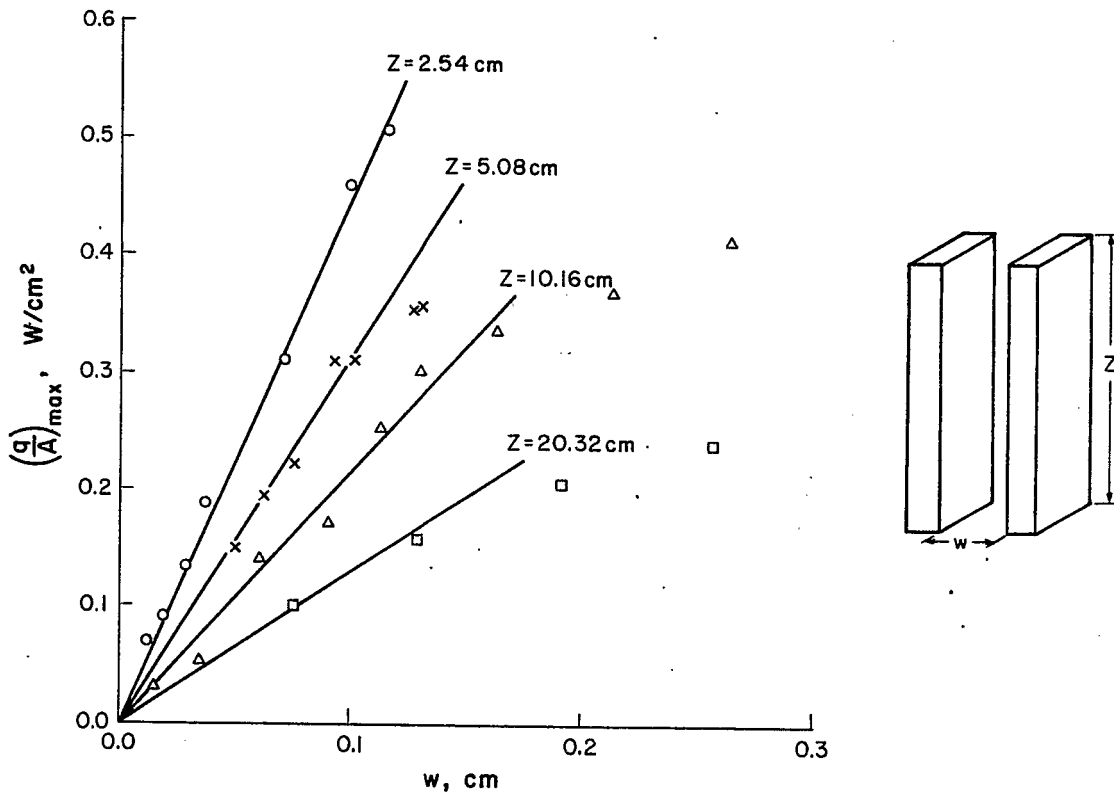


Fig. 19. Experimental data on helium boiling in vertical channels from Wilson (Ref. 52). Solid lines are maximum heat flux prediction from Sydoriak and Roberts (Ref. 51).

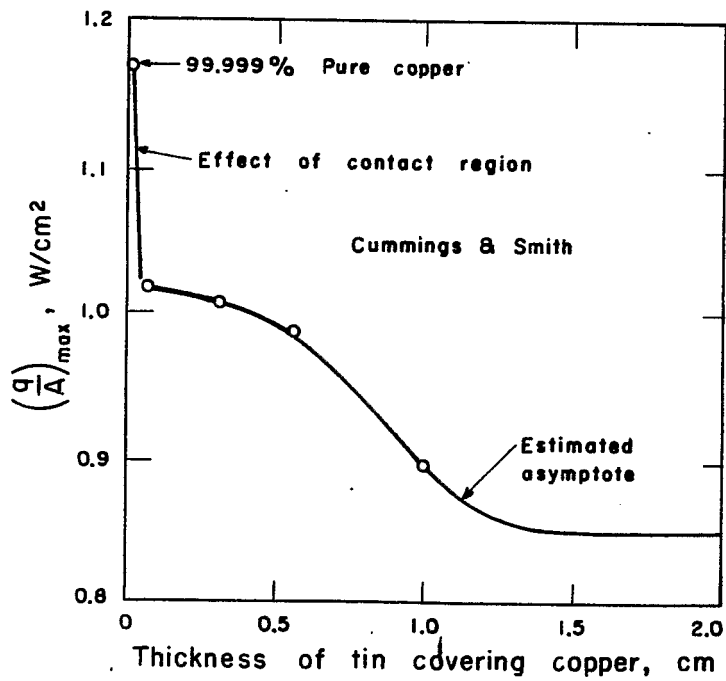


Fig. 20. Data for pool boiling of helium showing the effect of variations in the substrate material from Cummings and Smith (Ref. 40).

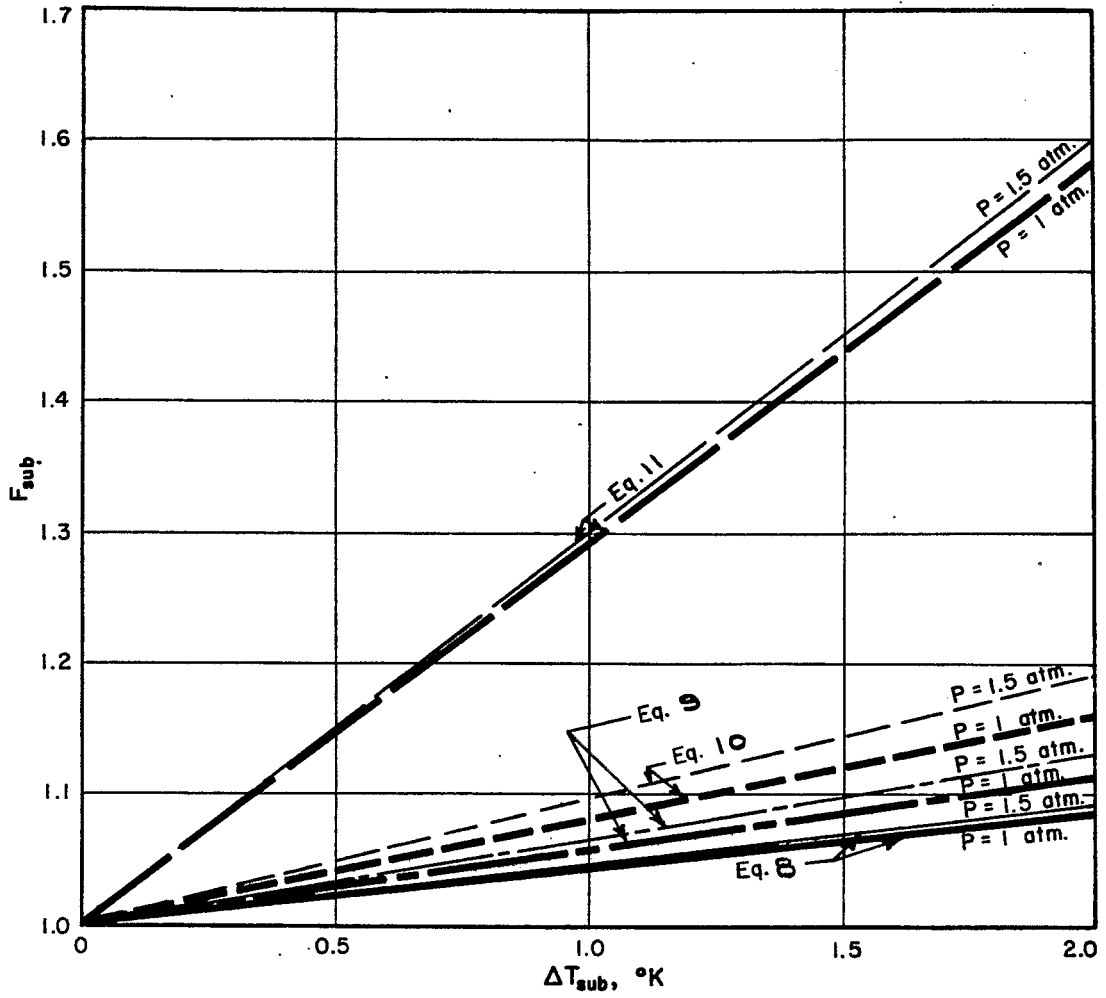


Fig. 21. Correction factor for maximum nucleate boiling flux for subcooled helium.

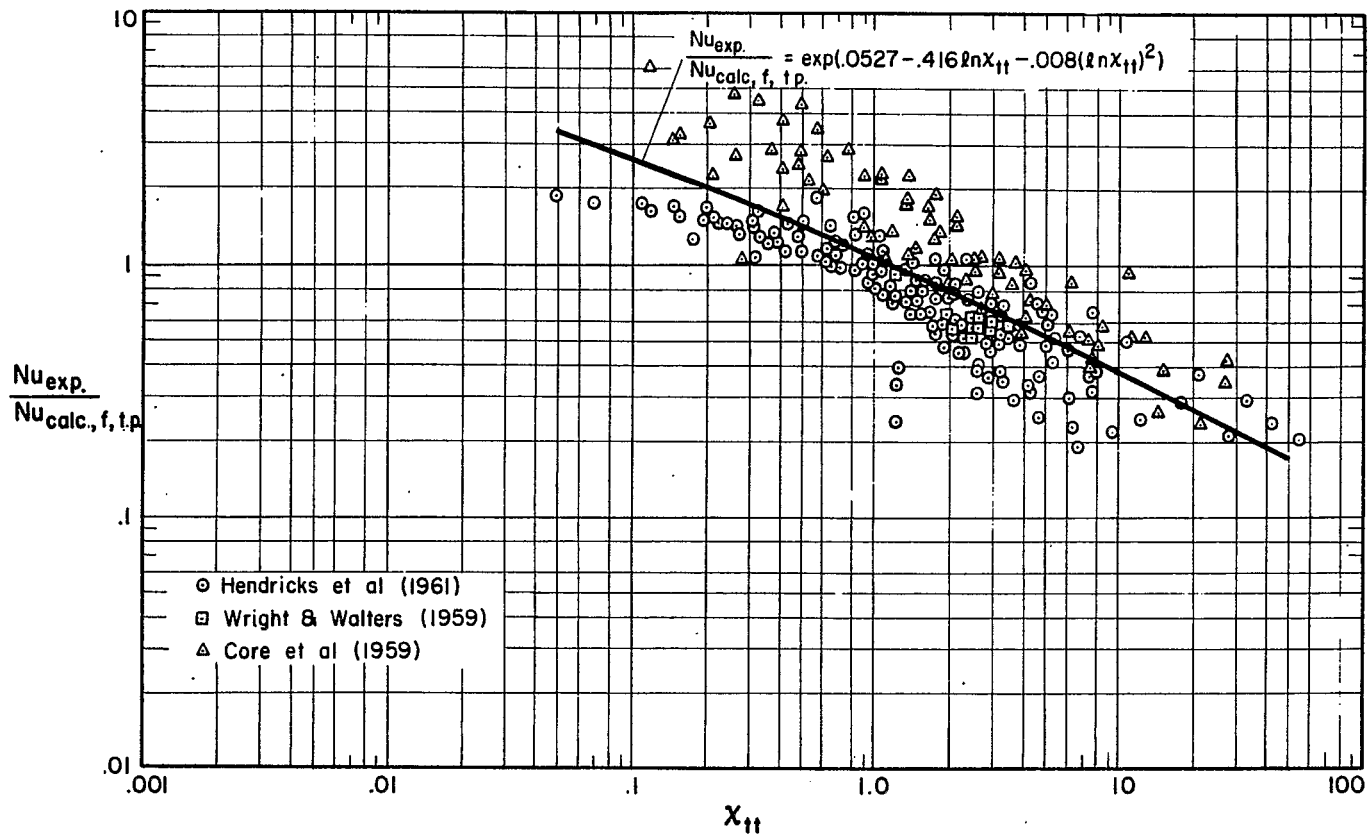


Fig. 22. Two-phase Nusselt number ratio vs x_{tt} for hydrogen. Correlation from Hendricks et al. (Ref. 17), figure from Brentari et al. (Ref. 56).

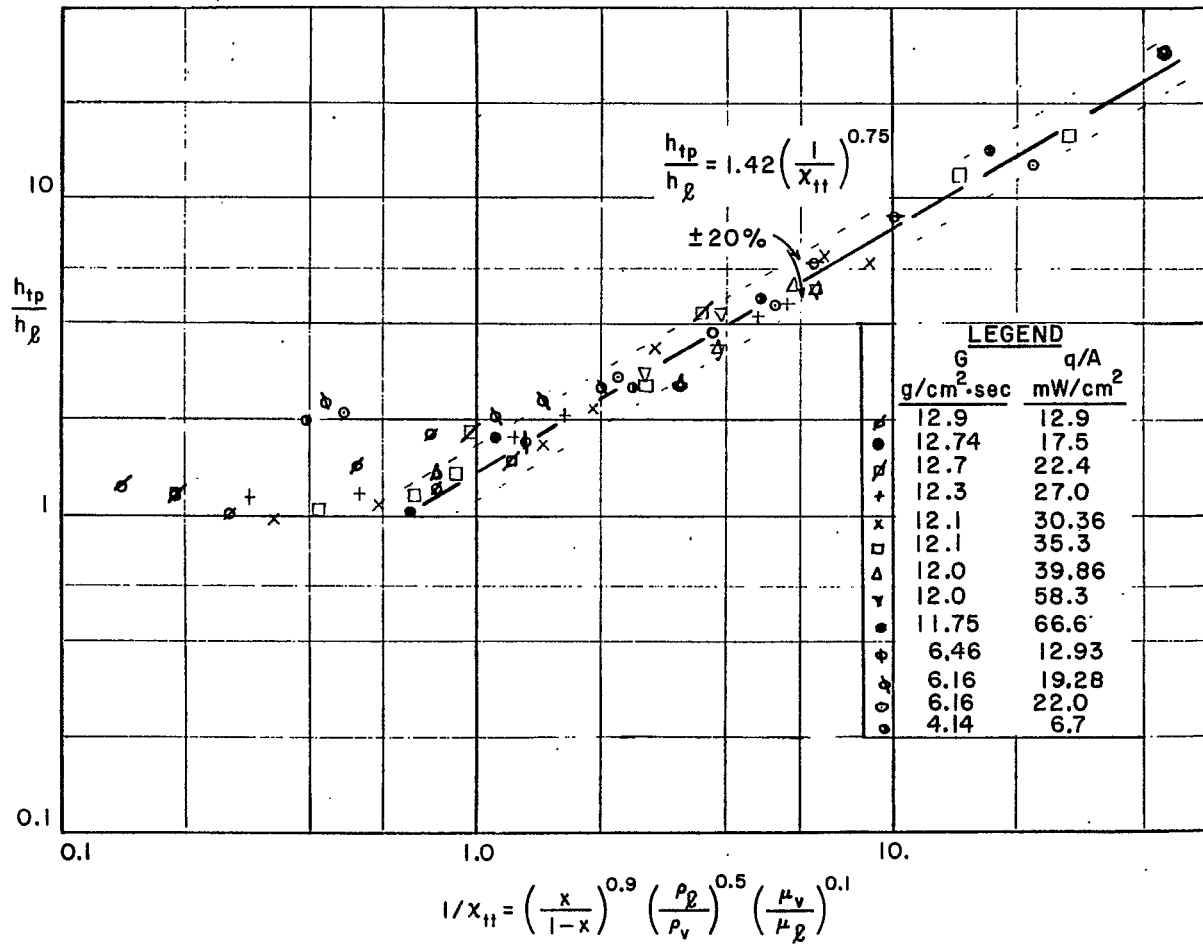


Fig. 23. Data for forced convection boiling of helium compared with a Martinelli-type correlation from de La Harpe et al. (Ref. 58).

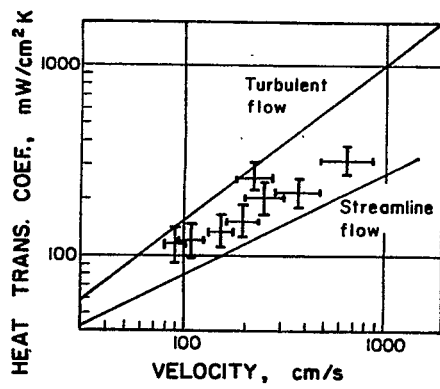


Fig. 24. Forced convection heat transfer data for liquid helium from Dorey (Ref. 60). Experimental data are compared with predicted results for streamline and turbulent flow.